Gravitational waves from a spinning particle plunging into a Kerr black hole

Motoyuki Saijo* and Kei-ichi Maeda†
Department of Physics, Waseda University, 3-4-1 Okubo, Shinjuku, Tokyo 169-8555, Japan

Masaru Shibata‡ and Yasushi Mino§
Department of Earth and Space Science, Osaka University, Toyonaka 560-0043, Japan
(Received 29 December 1997; published 5 August 1998)

Using a black hole (BH) perturbation approach, we numerically study gravitational waves from a spinning particle of mass μ and spin s on the equatorial plane plunging into a Kerr BH of mass M and spin a. When we take into account the particle spin s, (a) the motion of the particle changes due to the coupling effects between s and the orbital angular momentum L_z and between s and a, and also (b) the energy momentum tensor of the linearized Einstein equations changes. We calculate the total radiated energy, linear momentum, angular momentum, the energy spectrum, and waveform of gravitational waves, and we find the following features. (1) There are three spin coupling effects: between L_z and a, between s and L_z, and between s and a when s is considered. Among them, $(L_z \cdot a)$ coupling is the most important effect for the amount of gravitational radiation, and the other two effects are not as remarkable as the first one. However, these effects are still important; for example, the total radiated energy changes by a factor of ~ 2 for the case of $a/M=0.6$, $L_z/\mu M=1.5$ if we change s from 0 to $\lesssim M$. (2) For the case when one of the three spins (a, L_z, and s) is vanishing, the amount of gravitational radiation becomes larger (smaller) if spin axes of the other two are parallel (antiparallel). For the case when three spins are nonvanishing, the amount of gravitational radiation becomes maximum if all the axial directions of s, a, and L_z coincide. Thus, our calculations indicate that in a coalescence of two black holes (BHs) whose spins and orbital angular momentum are aligned, gravitational waves are emitted most efficiently. [S0556-2821(98)05216-3]

PACS number(s): 04.30.Db, 04.25.Nx

I. INTRODUCTION

Ground-based laser interferometers such as the Laser Interferometeric Gravitational Wave Observatory (LIGO) [1], VIRGO [2], GEO600 [3], and TAMA300 [4] will be in operation within the next five years. Among the many possible sources of gravitational waves, coalescing binaries composed of neutron stars (NSs) or black holes (BHs) are probably the most well-understood source, and are potentially among the most promising sources. In particular, merging binary BHs are expected to be the most general relativistic phenomena, and the detections of gravitational waves from them will enable us to obtain physical information in extremely curved spacetime. In order to extract it from a noisy data effectively, it is necessary to prepare in advance a list of theoretical templates of gravitational waves, which depend on many parameters of sources (masses, spins, quadrupole moments, and the orbital inclination of compact objects, and so on) [5].

A fully general relativistic simulation is the only method by which such templates can be prepared, and much effort is now being paid to such simulations [6]. We usually expect that the numerical simulation must be performed accurately throughout the large dynamic range from the innermost stable circular orbit to the final merging. To carry it out, there are many problems to be solved; e.g., we need to find appropriate gauge and slice conditions for 3D numerical relativity, to construct a sophisticated computational program for treating highly curved spacetime near BH horizons, and so on. Moreover, a huge amount of computational time will be necessary to perform many simulations for many possible parameters of BH binaries. Much progress in this field has been done in the last five years and will be expected in the next five years, but it will still be helpful if we could have another more reliable and economical approximate method to calculate gravitational waves from merging BH-BH binaries, because the result will be a guideline or a template in carrying out those fully general relativistic simulations.

A BH perturbation approach is one of approximate methods to calculate gravitational waves from merging binary BHs. In this approach, we assume that a small particle of mass μ is moving around the other large BH of mass $M \gg \mu$, and calculate gravitational waves emitted using linearized Einstein equations ignoring $O[(\mu/M)^2]$ terms in the BH spacetime as the background. The advantage of this approach is that it enables us to treat full general relativistic effects of the background BH spacetime and it may be applied to an arbitrary motion of a particle in principle. Although this approximation is valid only for $\mu \ll M$, we expect that the perturbation calculation will give a fairly good approximation to numerical relativistic calculations; in fact, the waveform and total radiated energy of gravitational waves in the head-on collision of two equal mass (m) BHs [7] agree with the extrapolated value ($M \to 2m$, $\mu \to m/2$) of those obtained by a perturbation calculation [8] with a fairly good accuracy (within a factor of 2). The waveforms obtained in the simulations of the stellar core collapse to be a BH [9]

*Electronic address: saijo@gravity.phys.waseda.ac.jp
†Electronic address: maeda@gravity.phys.waseda.ac.jp
‡Electronic address: shibata@vega.ess.sci.osaka-u.ac.jp
§Electronic address: mino@vega.ess.sci.osaka-u.ac.jp

also agree with those calculated by a perturbation study of a rotating ring inspiraling into a Schwarzschild BH [10].

Along this approach, many works have been carried out to study gravitational waves from a nonspinning test particle plunging into a spinning BH, since Sasaki and Nakamura [11] reformulated the Teukolsky equation [12] and made it possible to calculate gravitational waves induced by a particle plunging into a Kerr BH from infinity. (See Nakamura, Oohara, and Kojima [10].) To study gravitational waves from merging binaries of spinning BHs approximately, Mino, Shibata, and Tanaka [13] extended the Sasaki-Nakamura formalism incorporating the energy momentum tensor and the equations of motion of a spinning particle. They calculated gravitational waves from a spinning particle falling along the spin axis of a Kerr BH and showed that the effect of a particle spin is significant. In this paper, we investigate gravitational waves from a spinning particle moving on the equatorial plane plunging into a Kerr BH.

This paper is organized as follows. In Secs. II A, II B, and II C, we derive the explicit form of the equations of motion of a spinning particle moving on the equatorial plane of a Kerr BH. We also mention the limitation of the equations of motion in Sec. II C. In Sec. II D, we review the energy momentum tensor of a spinning particle. We present numerical results in Sec. III. Section IV is devoted to a conclusion. The detailed equations for a calculation of gravitational waves such as the generalized Regge-Wheeler equation (Sasaki-Nakamura equation), and its source terms are summarized in the Appendix. Throughout this paper, we use geometrized units in which $c=1=G$ and the metric sign as $(-,+,+,+)$.

II. THE MOTION OF A SPINNING PARTICLE

A. Equations of motion

The equations of motion of an extended body were first derived by Papapetrou [14] for a spinning particle case, and then reformulated by Dixon [15] for a general extended body. The equations of motion of a spinning particle are given as

$$\frac{D}{d\tau}p^{\mu}=-\frac{1}{2}R^{\mu}{}_{\nu\rho\sigma}(z)v^{\nu}S^{\rho\sigma},$$
$$\frac{D}{d\tau}S^{\mu\nu}=p^{\mu}v^{\nu}-p^{\nu}v^{\mu}, \tag{2.1}$$

where $z^{\mu}(\tau)$, $v^{\mu}(\tau)\equiv dz^{\mu}/d\tau$, $p^{\mu}(\tau)$, $S^{\mu\nu}(\tau)$, and $R^{\mu}{}_{\nu\rho\sigma}$ denote the world line, 4-velocity, momentum, spin angular momentum tensor of the spinning particle, and Riemann tensor of a Kerr spacetime, respectively, with τ being an affine parameter of the orbit. The quantity $\mu^2\equiv -p_{\mu}p^{\mu}$ is conserved along the orbit, and we regard it as the square of the mass of the particle. We also introduce a normalized momentum $u^{\mu}=p^{\mu}/\mu$. The notation $D/d\tau$ denotes the covariant derivative along the particle trajectory.

In order to close our system, we need a set of supplementary conditions, i.e., a relation between v^{μ} and u^{μ} (or p^{μ}), as [15]

$$S^{\mu\nu}p_{\nu}=0. \tag{2.2}$$

This relation fixes the center of mass of the spinning particle. The magnitude of spin is also conserved, so that we set

$$S^{\mu\nu}S_{\mu\nu}=2\mu^2s^2, \tag{2.3}$$

where a constant s is the specific spin angular momentum of the particle. For the latter convenience, we normalize the orbital affine parameter τ as

$$u^{\mu}v_{\mu}=-1. \tag{2.4}$$

Note that there is no *a priori* definition with regard to normalization of $v^{\mu}v_{\mu}$ besides the constraint that it must be negative. Using Eqs. (2.1), (2.2), and (2.4), the relation between u^{μ} and v^{μ} becomes

$$v^{\mu}-u^{\mu}=\frac{S^{\mu\nu}R_{\nu\gamma\sigma\lambda}u^{\gamma}S^{\sigma\lambda}}{2(\mu^2+\frac{1}{4}R_{\alpha\beta\delta\xi}S^{\alpha\beta}S^{\delta\xi})}. \tag{2.5}$$

Thus, Eqs. (2.1), (2.2), and (2.5) are equations to be solved.

B. Conserved quantities

Conserved quantities are often very useful to obtain the orbit in an explicit manner. If we have a Killing vector ξ_{μ} which satisfies $\xi_{\mu;\nu}+\xi_{\nu;\mu}=0$, the quantity

$$Q_{\xi}=p^{\mu}\xi_{\mu}-\tfrac{1}{2}S^{\mu\nu}\xi_{\mu;\nu}, \tag{2.6}$$

is conserved along a particle trajectory [15].

Apart from the mass μ and spin s of a spinning particle, we have two additional conserved quantities because in Kerr spacetime, there are two Killing vectors [16]: One is a timelike Killing vector ξ_{μ} given by

$$\xi_{\mu}=-\left(\sqrt{\frac{\Delta}{\Sigma}}e^{(0)}_{\mu}+\frac{a\sin\theta}{\sqrt{\Sigma}}e^{(3)}_{\mu}\right), \tag{2.7}$$

and the other is an axial Killing vector χ_{μ} given by

$$\chi_{\mu}=a\sqrt{\frac{\Delta}{\Sigma}}\sin^2\theta e^{(0)}_{\mu}+\frac{(r^2+a^2)\sin\theta}{\sqrt{\Sigma}}e^{(3)}_{\mu}, \tag{2.8}$$

where a is a spin parameter of the Kerr BH, $\Delta\equiv r^2-2Mr+a^2$, and $\Sigma\equiv r^2+a^2\cos^2\theta$, respectively. We choose the tetrad bases of a covariant vector $e^{(a)}_{\mu}$ as

$$
\begin{aligned}
e^{(0)}_{\mu}dx^{\mu} &= \sqrt{\frac{\Delta}{\Sigma}}(dt - a\ \sin^2\ \theta d\phi),\\
e^{(1)}_{\mu}dx^{\mu} &= \sqrt{\frac{\Sigma}{\Delta}}dr,\\
e^{(2)}_{\mu}dx^{\mu} &= \sqrt{\Sigma}d\theta,\\
e^{(3)}_{\mu}dx^{\mu} &= \frac{\sin\ \theta}{\sqrt{\Sigma}}[-adt + (r^2+a^2)d\phi],
\end{aligned}
\tag{2.9}
$$

where quantities with Latin index denote their tetrad components. Then, two conserved quantities, the energy E, and the z component of the total angular momentum J_z of the particle, are given by

$$
\begin{aligned}
\frac{E}{\mu} &= -u^{\mu}\xi_{\mu} + \frac{1}{2\mu}S^{\mu\nu}\xi_{\mu;\nu}\\
&= \sqrt{\frac{\Delta}{\Sigma}}u^{(0)} + \frac{a\ \sin\ \theta}{\sqrt{\Sigma}}u^{(3)}\\
&\quad + \frac{M(r^2 - a^2\ \cos^2\ \theta)}{\Sigma^2}\frac{S^{(1)(0)}}{\mu} + \frac{2Mar\ \cos\ \theta}{\Sigma^2}\frac{S^{(2)(3)}}{\mu},
\end{aligned}
\tag{2.10}
$$

$$
\begin{aligned}
\frac{J_z}{\mu} &= u^{\mu}\chi_{\mu} - \frac{1}{2\mu}S^{\mu\nu}\chi_{\mu;\nu}\\
&= a\ \sin^2\ \theta\sqrt{\frac{\Delta}{\Sigma}}u^{(0)} + \frac{(r^2+a^2)\sin\ \theta}{\sqrt{\Sigma}}u^{(3)}\\
&\quad + \frac{a\ \sin^2\ \theta}{\Sigma^2}[(r-M)\Sigma + 2Mr^2]\frac{S^{(1)(0)}}{\mu}\\
&\quad + \frac{a\sqrt{\Delta}\ \sin\ \theta\ \cos\ \theta}{\Sigma}\frac{S^{(2)(0)}}{\mu} + \frac{r\sqrt{\Delta}\ \sin\ \theta}{\Sigma}\frac{S^{(1)(3)}}{\mu}\\
&\quad + \frac{\cos\ \theta}{\Sigma^2}[(r^2+a^2)^2 - a^2\Delta\ \sin^2\ \theta]\frac{S^{(2)(3)}}{\mu}.
\end{aligned}
$$

C. Equations of motion on the equatorial plane

In the following section, we restrict our analysis to the case, where a spinning particle moves on the equatorial plane of a Kerr BH ($\theta = \pi/2$). From this constraint, we find that the spin direction of a spinning particle is always perpendicular to the equatorial plane. To confirm this, we introduce a specific spin vector $s^{(a)}$ [17] as

$$
s^{(a)} = -\frac{1}{2\mu}\epsilon^{(a)}{}_{(b)(c)(d)}u^{(b)}S^{(c)(d)}, \tag{2.11}
$$

or equivalently,

$$
S^{(a)(b)} = \mu\epsilon^{(a)(b)}{}_{(c)(d)}u^{(c)}s^{(d)}, \tag{2.12}
$$

where $\epsilon_{(a)(b)(c)(d)}$ is the completely antisymmetric tensor with $\epsilon_{(0)(1)(2)(3)} = 1$. When the particle always moves on the equatorial plane of the Kerr BH, we find from the equations of motion [Eqs. (2.1)] that the nonvanishing component of the specific spin vector is only $s^{(2)}$. Then we set $s^{(2)} = -s$, where s indicates not only the magnitude of a particle spin, but also includes the information of a spin direction, i.e., the particle spin is parallel to the BH spin for $s > 0$, while it is antiparallel for $s < 0$.

From Eq. (2.12), nonvanishing tetrad components of the spin angular momentum are obtained as

$$
\begin{aligned}
S^{(0)(1)} &= -\mu s u^{(3)},\\
S^{(0)(3)} &= \mu s u^{(1)},\\
S^{(1)(3)} &= \mu s u^{(0)},
\end{aligned}
\tag{2.13}
$$

and the conserved energy and total angular momentum [Eq. (2.10)] can be written as

$$
\begin{aligned}
\frac{E}{\mu} &= \frac{\sqrt{\Delta}}{r}u^{(0)} + \frac{(ar+Ms)}{r^2}u^{(3)},\\
\frac{J_z}{\mu} &= \frac{\sqrt{\Delta}}{r}(a+s)u^{(0)} + \left[\frac{(r^2+a^2)}{r} + \frac{as}{r^2}(r+M)\right]u^{(3)}.
\end{aligned}
\tag{2.14}
$$

Using Eqs. (2.5), (2.14), and the normalization $u^{\mu}u_{\mu} = -1$, the relation between the normalized momentum vector $u^{(a)}$ and the 4-velocity $v^{(a)}$ are

$$
v^{(0)} = N\left(1 - \frac{Ms^2}{r^3}\right)u^{(0)}, \tag{2.15}
$$

$$
v^{(1)} = N\left(1 - \frac{Ms^2}{r^3}\right)u^{(1)}, \tag{2.16}
$$

$$
v^{(3)} = N\left(1 + \frac{2Ms^2}{r^3}\right)u^{(3)}, \tag{2.17}
$$

where

$$
N = \left(1 - \frac{Ms^2}{r^3}[1 + 3(u^{(3)})^2]\right)^{-1}. \tag{2.18}
$$

Then, we can derive explicit components of velocity fields from Eqs. (2.14)–(2.17) as

$$
\Sigma_s\Lambda_s\frac{dt}{d\tau} = a\left(1 + \frac{3Ms^2}{r\Sigma_s}\right)[\tilde{J}_z - (a+s)\tilde{E}] + \frac{r^2+a^2}{\Delta}P_s, \tag{2.19}
$$

$$
\Sigma_s\Lambda_s\frac{dr}{d\tau} = -\sqrt{R_s}, \tag{2.20}
$$

$$\Sigma_s \Lambda_s \frac{d\varphi}{d\tau} = \left(1 + \frac{3Ms^2}{r\Sigma_s}\right)[\tilde{J}_z - (a+s)\tilde{E}] + \frac{a}{\Delta} P_s, \tag{2.21}$$

where

$$\Sigma_s = r^2\left(1 - \frac{Ms^2}{r^3}\right), \tag{2.22}$$

$$\Lambda_s = 1 - \frac{3Ms^2 r[-(a+s)\tilde{E} + \tilde{J}_z]^2}{\Sigma_s^3}, \tag{2.23}$$

$$R_s = P_s^2 - \Delta\left(\frac{\Sigma_s^2}{r^2} + [-(a+s)\tilde{E} + \tilde{J}_z]^2\right), \tag{2.24}$$

$$P_s = \left((r^2+a^2) + \frac{as}{r}(r+M)\right)\tilde{E} - \left(a + \frac{Ms}{r}\right)\tilde{J}_z, \tag{2.25}$$

and the energy and total angular momentum of the spinning particle were normalized as $\tilde{E} \equiv E/\mu$ and $\tilde{J}_z \equiv J_z/\mu$, respectively. Since we pay attention only to the case when the particle plunges into the BH, we choose the minus sign in the right-hand side of Eq. (2.20).

One can easily understand the property of the radial motion of a particle by using an effective potential [18]. We rewrite Eq. (2.24) to an equation for E as

$$\alpha E^2 - 2\beta E + \gamma - (\Sigma_s p^r)^2 = 0, \tag{2.26}$$

where $p^r = \mu u^r$, and

$$\alpha = \left((r^2+a^2) + \frac{as}{r}(r+M)\right)^2 - \Delta(a+s)^2,$$

$$\beta = \left[\left(a + \frac{Ms}{r}\right)\left((r^2+a^2) + \frac{as}{r}(r+M)\right) - \Delta(a+s)\right] J_z,$$

$$\gamma = \left(a + \frac{Ms}{r}\right)^2 J_z^2 - \Delta\left[r^2\left(1 - \frac{Ms^2}{r^3}\right)^2 + J_z^2\right].$$

The effective potential is defined as the minimum allowed value of the particle energy at radius r; i.e.,

$$V_{\rm eff} = \frac{\beta + \sqrt{\beta^2 + \alpha\gamma}}{\alpha}, \tag{2.27}$$

where we take the positive square root because the motion of a spinning particle should be future directed. We show this effective potential in Fig. 1 for some sets of parameters. Here, we note that there may appear the following pathological feature in treating the equations of motion of a spinning particle: As mentioned in Sec. II A, for the case $s \neq 0$, there is no normalization relation for $v^\mu v_\mu$, and hence the timelike condition $v^\mu v_\mu < 0$ is not guaranteed in the equations of motion of a spinning particle. In reality, for the case where s is large enough, $v^\mu v_\mu$ becomes positive for some choices E and J_z [see Fig. 1(d)]. Hence, we have to incorporate the timelike condition for v^μ additionally. Using Eqs. (2.14)–(2.17), the timelike condition, $v^\mu v_\mu < 0$, is reduced to the inequality

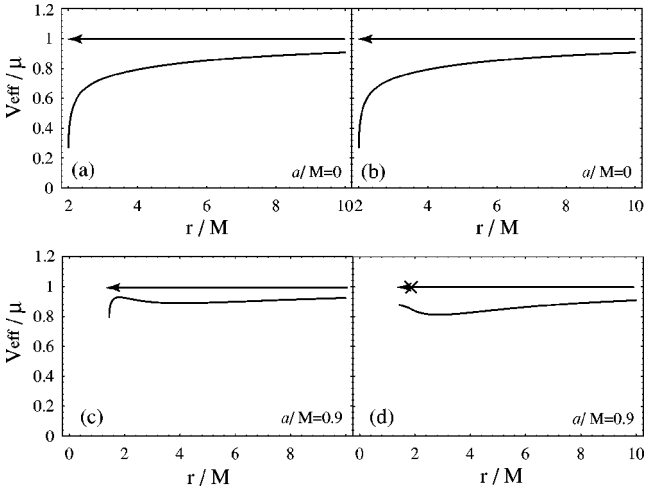

FIG. 1. The effective potential [Eq. (2.27)] of a spinning particle moving on the equatorial plane for (a) $(a/M, s/M, L_z/\mu M) = (0,0,2.4)$, (b) $(0,0.9,1.5)$ (c), $(0.9,0,2.4)$, and (d) $(0.9,0.9,1.5)$, where $L_z = J_z - \mu s$ [see Eq. (3.1)]. Note that J_z is fixed to be $2.4\mu M$. The arrows indicate the trajectories of a spinning particle. Figure 1(d) shows the case, where the timelike condition along the particle trajectory is violated, and we mark the cross point at which $v^\mu v_\mu = 0$.

$$3\frac{[\tilde{J}_z - \tilde{E}(a+s)]^2}{(Ms^2)^{2/3}} < \frac{(1-X)^4}{(2+X)X^{5/3}}, \tag{2.28}$$

where $X \equiv Ms^2/r^3$. This condition must be satisfied for any value of $r \geqslant r_H$, where r_H denotes the coordinate radius of event horizon ($r_H \equiv M + \sqrt{M^2 - a^2}$) [19]. We depict this con-

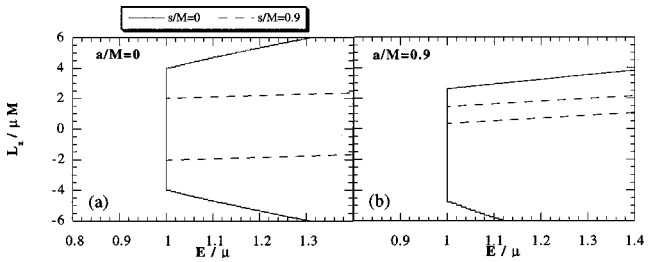

FIG. 2. The allowed region of parameters (E, L_z) for a particle to fall from infinity into a BH [(a) $a/M = 0$, (b) $a/M = 0.9$]. The quantities E and L_z represent the energy and the orbital angular momentum of a spinning particle, respectively. The allowed regions of E, L_z are encompassed by solid $(s/M = 0)$ and dashed lines $(s/M = 0.9)$, respectively. (Note that along $E/\mu = 1$, dashed line lies below solid one.)

TABLE I. Allowed region of the ''orbital angular momentum'' of the spinning particle ($L_{z\,\min}<L_z<L_{z\,\max}$) which is constrained by the timelike condition of its trajectory. We defined the orbital angular momentum L_z as $L_z=J_z-\mu s$ [See Eq. (3.1)]. Since we consider only the case of zero radial velocity at infinity, we only show the case of $E=\mu$ in this table.

a/M	s/M	$L_{z\,\min}/\mu M$	$L_{z\,\max}/\mu M$
0.0	0.3	−7.505	7.505
	0.6	−3.472	3.472
	0.9	−2.022	2.022
0.3	0.3	−6.767	7.367
	0.6	−2.950	3.550
	0.9	−1.538	2.173
0.6	0.3	−5.112	6.312
	0.6	−1.965	3.165
	0.9	−0.814	2.014
0.9	0.3	−2.237	4.037
	0.6	−0.359	2.159
	0.9	0.345	1.455

dition in Figs. 2. We find that the allowed region is highly constrained when the spin is large ($s/M\sim 1$) and no plunging orbit is allowed for $a/M=s/M=1$. We also summarize the allowed region from the timelike condition in Table I with $E=\mu$, for which we perform our analysis in this paper.

We guess that there cannot be such a pathological orbit in a realistic situation, and that appearance of such an orbit might be due to the violation of the assumption in deriving basic equations in this extreme situation. The equations of motion of a spinning particle were derived under the assumption that its characteristic radius (or magnitude of spin s) is much smaller than the curvature scale of a background spacetime. Hence, if a particle spin s is much smaller than a horizon radius r_H when the particle plunges into a BH [20], no pathological feature appears.

Exactly speaking, results presented in the following are reliable only for $|s|/r_H \lesssim |s|/M \ll 1$, as mentioned above. However, it is interesting to extend the analysis to the case $|s|\sim M$ because the result could be helpful for understanding the feature of gravitational waves from coalescence of a highly spinning binary BHs. Therefore, in this paper, we consider the case, where $|s|/M\sim O(1)$, unless the timelike condition is violated. When the timelike condition is violated for a set of parameters (s,E,J_z) somewhere before a spinning particle reaches r_H, we simply exclude the case.

D. Energy-momentum tensor of a spinning particle

As the source term of Einstein equations, we use the energy momentum tensor of a spinning particle $T^{\mu\nu}$, which is given as [13]

$$T^{\mu\nu}(x)=\frac{1}{\sqrt{-g}}\int d\tau\Big[p^{(\mu}(x,\tau)v^{\nu)}(x,\tau)\,\delta^{(4)}(x-z(\tau)) - \nabla_\lambda S^{\lambda(\mu}(x,\tau)v^{\nu)}(x,\tau)\,\delta^{(4)}(x-z(\tau))\Big], \quad (2.29)$$

where $v^\alpha(x,\tau)$, $p^\alpha(x,\tau)$, and $S^{\alpha\beta}(x,\tau)$ are defined extensively from $v^\mu(\tau)$, $p^\mu(\tau)$, and $S^{\mu\nu}(\tau)$, which are defined only on the particle trajectory. These extended fields are defined only around the particle trajectory $x^\mu=z^\mu(\tau)$ [21], using a bivector of parallel displacement $\overline{g_\mu}^{\,\alpha}(x,z)$ [22] defined as

$$\lim_{x\to z}\overline{g_\mu}^{\,\alpha}(x,z(\tau))=\delta_\mu{}^\alpha, \qquad \lim_{x\to z}\nabla_\beta\overline{g_\mu}^{\,\alpha}(x,z(\tau))=0. \quad (2.30)$$

For the present case (with a mass monopole and a spin dipole moment), a further specification of $\overline{g^\alpha}_\mu(x,z)$ is not required. Using the bivector $\overline{g^\alpha}_\mu(x,z)$, we define $v^\alpha(x,\tau)$, $p^\alpha(x,\tau)$, and $S^{\alpha\beta}(x,\tau)$ as

$$v^\alpha(x,\tau)=\overline{g^\alpha}_\mu(x,z(\tau))v^\mu(\tau), \qquad p^\alpha(x,\tau)=\overline{g^\alpha}_\mu(x,z(\tau))p^\mu(\tau), \qquad S^{\alpha\beta}(x,\tau)=\overline{g^\alpha}_\mu(x,z(\tau))\overline{g}_\nu{}^\beta(x,z(\tau))S^{\mu\nu}(\tau). \quad (2.31)$$

From these equations, we can get the energy-momentum tensor without ambiguity.

Using Eqs. (2.31) with the relations

$$\nabla_\beta\overline{g^\alpha}_\mu(x,z(\tau))\,\delta^{(4)}(x,z(\tau))=0, \qquad v^\alpha(x)\nabla_\alpha\left(\frac{\delta^{(4)}(x,z(\tau))}{\sqrt{-g}}\right)=-\frac{d}{d\tau}\left(\frac{\delta^{(4)}(x,z(\tau))}{\sqrt{-g}}\right), \quad (2.32)$$

the divergence of Eq. (2.29) can be written as

$$\nabla_\beta T^{\alpha\beta}(x)=\int d\tau\overline{g^\alpha}_\mu(x,z(\tau))\frac{\delta^{(4)}(x,z(\tau))}{\sqrt{-g}}\left(\frac{d}{d\tau}p^\mu(\tau)+\frac{1}{2}R^\mu{}_{\nu\rho\sigma}(z(\tau))v^\nu(\tau)S^{\rho\sigma}(\tau)\right) + \frac{1}{2}\int d\tau\nabla_\beta\left(\overline{g^\alpha}_\mu(x,z(\tau))\overline{g}^\beta{}_\nu(x,z(\tau))\frac{\delta^{(4)}(x,z(\tau))}{\sqrt{-g}}\right)\left(\frac{d}{d\tau}S^{\mu\nu}(\tau)-2p^{[\mu}(\tau)v^{\nu]}(\tau)\right). \quad (2.33)$$

Thus, by the equations of motion (2.1), the divergence free condition $\nabla_\mu T^{\mu\nu}=0$ is guaranteed.

III. GRAVITATIONAL WAVES FROM A SPINNING PARTICLE

To investigate gravitational waves emitted from a spinning particle plunging into a Kerr BH, we adopt the Sasaki-Nakamura formalism [11]. In order to calculate the total radiated energy ΔE, energy spectrum $(dE/d\omega)_{lm\omega}$ and so on using their formalism, we need to obtain source terms $\mathcal{S}_{lm\omega}(r)$ which consists of the motion of a spinning particle, to integrate the radial wave equation for $X_{lm\omega}(r)$, and to construct the waveforms h_+ and $h_\times$. In the Appendix, we summarize the basic equations required. In this section, we only present numerical results and discuss implication of them.

For a nonspinning test particle plunging into a BH, we have learned that an orbital angular momentum L_z, which is a conserved quantity, is one of the most important key parameters in determining the amount of gravitational radiation [10]. In the case of a spinning particle, however, we just have the total angular momentum J_z and do not have an ''orbital angular momentum'' *a priori.* Here, we introduce an ''orbital angular momentum'' at infinity as

$$L_z = J_z - \mu s, \tag{3.1}$$

and hereafter use it as a parameter of our analysis for gravitational waves instead of J_z.

A. Effects of a particle spin, black hole spin, and orbital angular momentum to the total radiated energy of gravitational waves

In Figs. 3 and 4, we show the total radiated energy ΔE for a wide variety of parameters. In Figs. 3, we show ΔE as a function of L_z fixing $a/M(=0,0.3,0.6,0.9)$ and $s/M(=0, \pm 0.9)$, and in Figs. 4, ΔE as a function of a and s fixing $L_z/\mu M$ as $0, \pm 1.5$ and ± 3. In these figures, we may find the less number of data points for larger s. This is because of the violation of the timelike condition on v^μ for large s.

First, we pay attention to a Schwarzschild BH case, where $a=0$ (see, e.g., Fig. 3(a) or Figs. 4 along s axis). In this case, we can find the following features: (1) The total radiated energy ΔE is sensitively dependent on L_z. With increasing L_z, ΔE increases by a factor of 10 for very large $|L_z|/\mu M \sim 3.5$. (2) The effect of s is not as remarkable as that of L_z, but it changes the amount of gravitational radiation by a factor of 2. (3) In the case, where s and L_z are parallel, ΔE is always larger than in the case when they are antiparallel.

We guess that the features (1)–(3) may be roughly understood by considering the trajectories of the particle: For the case where $|L_z|$ is larger, the particle stays in the strong gravitational field region for a longer time due to the centrifugal force $\propto L_z^2/r^3$. Since a particle emits most of gravitational waves when it stays in a strong gravitational field region near the event horizon, the particle emits much more gravitational waves for larger $|L_z|$.

A similar idea can also be applied to interpreting the features (2) and (3). If s and L_z are parallel (antiparallel), the particle stays in a strong gravitational field region for a longer (shorter) time compared with the case of $s=0$ due to

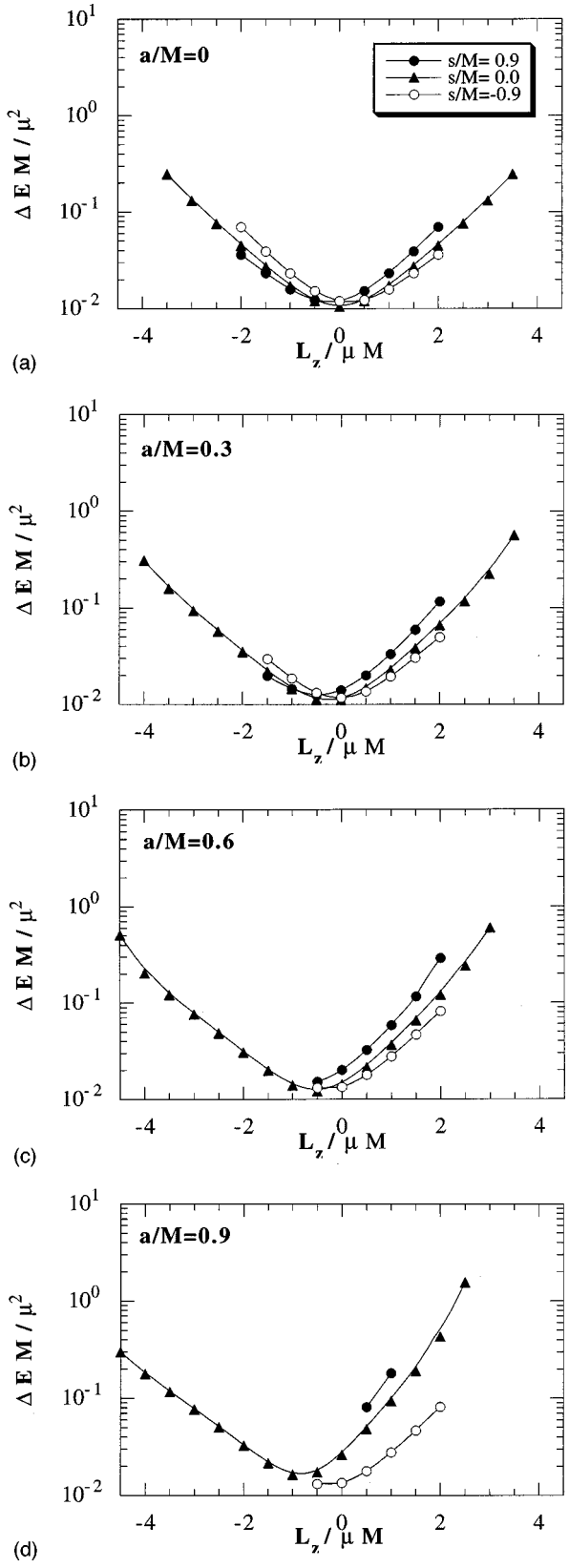

FIG. 3. The total radiated energy of gravitational waves as a function of L_z [(a) $a/M=0$, (b) $a/M=0.3$, (c) $a/M=0.6$, and (d) $a/M=0.9$]. Circle (filled), triangle (filled), and circle (open) denote the cases of $s/M=0.9$, 0, and -0.9, respectively.

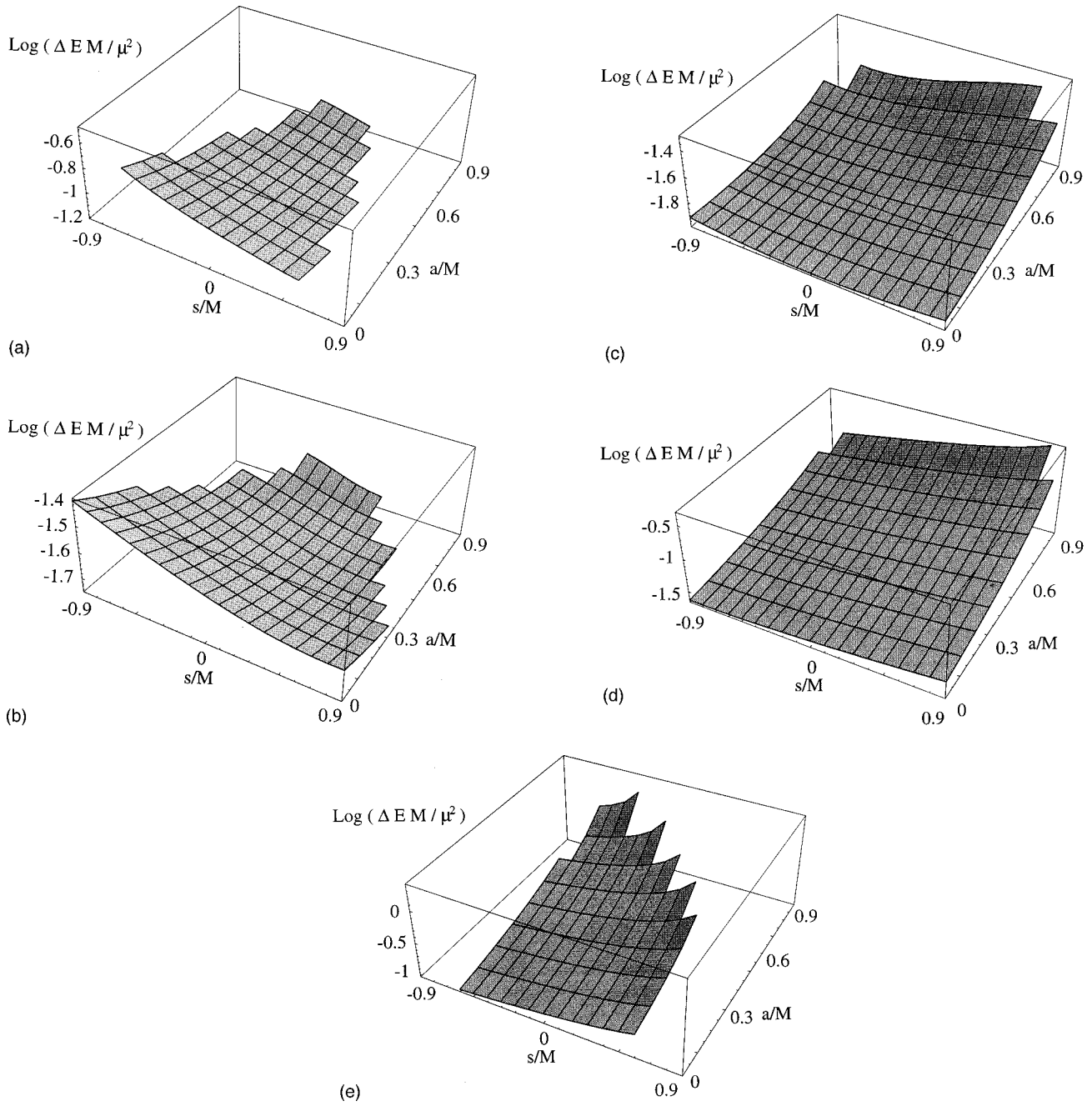

FIG. 4. The total radiated energy of gravitational waves as a function of a BH spin a and a particle spin s [(a) $L_z/\mu M=-3$, (b) $L_z/\mu M=-1.5$, (c) $L_z/\mu M=0$, (d) $L_z/\mu M=1.5$, and (e) $L_z/\mu M=3$].

the spin-orbit (SO) coupling force $\propto L_z sM/r^4$. Hence, when the direction of a particle spin is parallel (antiparallel) to L_z, more (less) gravitational waves are thought to be emitted than when a particle is nonspinning. Along this line, we may understand that the effect of s is not as remarkable as that of L_z since the spin-orbit (SO) coupling force is weaker than the centrifugal force by a factor of $|sM/L_z r|$.

Next, we consider a spinning BH case in which $a\neq 0$. We here begin with a discussion of the $s=0$ case and have a brief review of the previous argument in [10]. From our perturbation study, one may find the following features: (4) The value L_z, which makes the radiated energy minimum, shifts to a negative value of L_z for $a>0$ [see Figs. 3(b)–(d)]. (5) The increase rate of a radiated energy with increasing $|L_z|$ becomes larger for $L_z>0$ than that for $L_z<0$ [see Figs. 3(b)–(d)]. (6) Fixing $L_z\gtrsim 0$ ($L_z<0$), ΔE usually increases (decreases) as a increases.

The feature (4) is thought to be due to the frame-dragging effect of a Kerr BH. Around a Schwarzschild BH ($a=0$), the amount of gravitational radiation for a particle of $L_z=0$ is minimum since it has no toroidal motion. However, in a Kerr BH ($a>0$), the frame-dragging effect generates an ef-

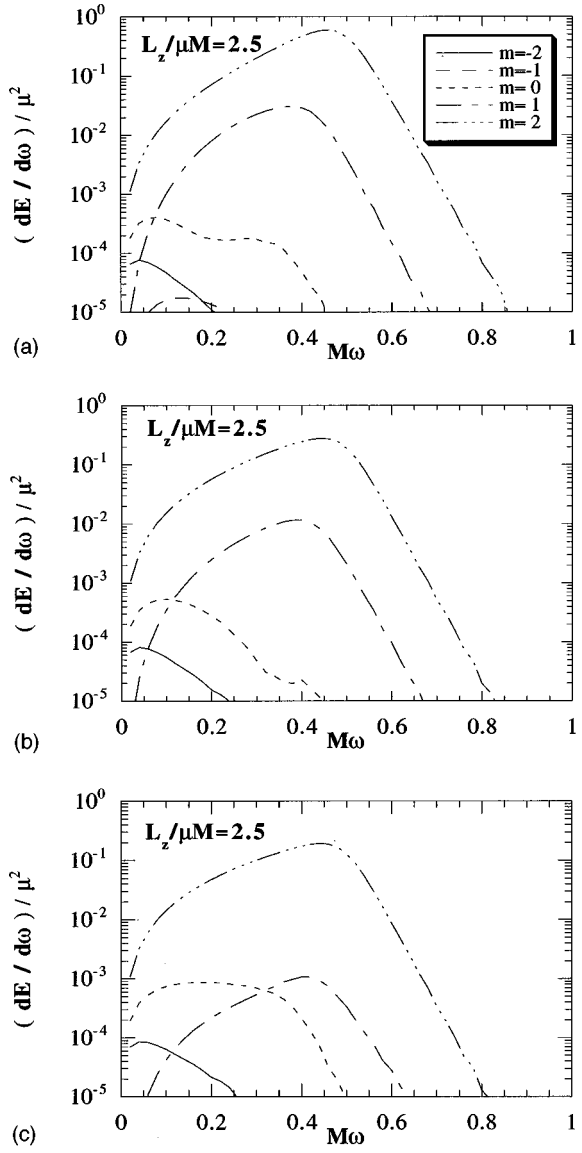

FIG. 5. The energy spectrum of gravitational waves of the $l=2$ mode for the case of $a/M=0.6$ and $L_z/\mu M=2.5$ [(a) $s/M=0.6$, (b) $s/M=0$, (c) $s/M=-0.6$]. Solid, dashed, dotted, dash-dotted, and dash-three dotted lines denote the cases of $m=-2$, -1, 0, 1, and 2, respectively.

fective toroidal motion. Thus a particle of $L_z<0$ could cancel this additional toroidal motion and radiate less energy than the particle of $L_z=0$.

The feature (5) might be understood in the same manner as we understand the feature (3). There exists a significant coupling between L_z and a, and in the case where L_z and a are parallel (antiparallel), the particle stays longer (shorter) around the horizon. As a result, ΔE is enhanced (reduced). Moreover, the wave propagation character in a Kerr background leads to this feature. The emissivity of gravitational waves significantly depends on the ringing tail of gravitational waves. For $L_z>0$, the $m=l$ mode dominates in the ringing tail, and the $m=-l$ mode dominates for $L_z<0$ (see Figs. 5–7 below). The quasinormal mode frequencies of a Kerr BH with $a/M=0.9$ are $M\omega=0.9-0.04i$ $(m=l=2)$ and $0.3-0.09i$ $(m=-l=-2)$, respectively [23]. Thus, the damping rate of the latter mode is considerably larger than the former one. This is the main reason why ΔE is larger for $L_z>0$ than for $L_z<0$. The explanation of the feature (6) might be essentially the same as that of (5). The damping rate of the ringing tail decreases with increasing a for $L_z \gtrsim 0$, and opposite relation holds for $L_z<0$.

Now, we discuss the effect of a particle spin s which first appears in this paper. For a Kerr background, there exist a coupling effect between a particle spin s and a BH spin a as a new effect, which we will call the spin-spin (SS) coupling.

We first consider the SO coupling between s and L_z for $a\neq 0$ [see, e.g., Figs. 4(d) and (e)]. As in the case $a=0$, ΔE increases (decreases) as s becomes larger for $L_z>0$ ($L_z<0$), however, the effect is significantly enhanced for a larger a. For example, from Fig. 4(d), ΔE for $a/M=0.9$ and $s/M=0.6$ is about ten times larger than that for $a=0$ and $s/M=0.6$, in the case of $L_z/\mu M=1.5$. This seems to show the importance of the coupling between a and the SO coupling term $(s\cdot L_z)$, and clearly implies that for the case, where their directions of axes have a coincidence, the amount of gravitational radiation becomes maximum.

The effect of the SS coupling can be seen from Fig. 4(c) in the case of $L_z=0$. We find that ΔE increases as a becomes larger for $s>0$ (or as s becomes larger for $a>0$). Thus, the SS coupling increases ΔE if the direction of two spin axes have a coincidence. This can also be seen for $L_z>0$ [see, e.g., Fig. 4(e)] as an enhancement effect. However, for $L_z<0$ [see, e.g., Fig. 4(a)], such an effect is not clear because the SO coupling is larger than the SS coupling, and makes it obscure to see SS coupling effect.

B. The linear momentum and angular momentum of gravitational waves

In Figs. 8 and 9, we show the total radiated linear momentum $\Delta|P|$ as a function of a, s, and L_z. The parameter dependence of $\Delta|P|$ is quite similar to that of ΔE as a whole. For example, in a Schwarzschild BH case, as $|L_z|$ increases, $\Delta|P|$ gets larger. Also, the SO coupling increases (decreases) $\Delta|P|$ for $(s\cdot L_z)>0(<0)$. However, the result seems to show that the SS coupling effect acts in the opposite sense: From Fig. 9(c), $\Delta|P|$ increases as $-(s\cdot a)$ gets large in the case, where $L_z=0$.

Total radiated angular momentum ΔJ_z as a function of a, s, and L_z are shown in Figs. 10 and 11. Again, the parameter dependence of ΔJ_z is similar to that of ΔE. However, there is one interesting feature: From the comparison of Figs. 3 and 10, for the critical orbital angular momentum $L_{z\,\mathrm{crit}}$ at which ΔE takes a minimum value, ΔJ_z becomes almost zero. This coincidence seems to be very reasonable from our interpretation of the feature (4) in a previous subsection. Since there is no effective toroidal motion at $L_z=L_{z\,\mathrm{crit}}$, a particle plunges into a Kerr BH along the most straight path and the angular momentum can hardly be radiated.

C. Energy spectrum and waveforms

In Figs. 5–7, we show the energy spectrum of gravitational waves of $l=2$ and $m=-2\sim 2$ modes.

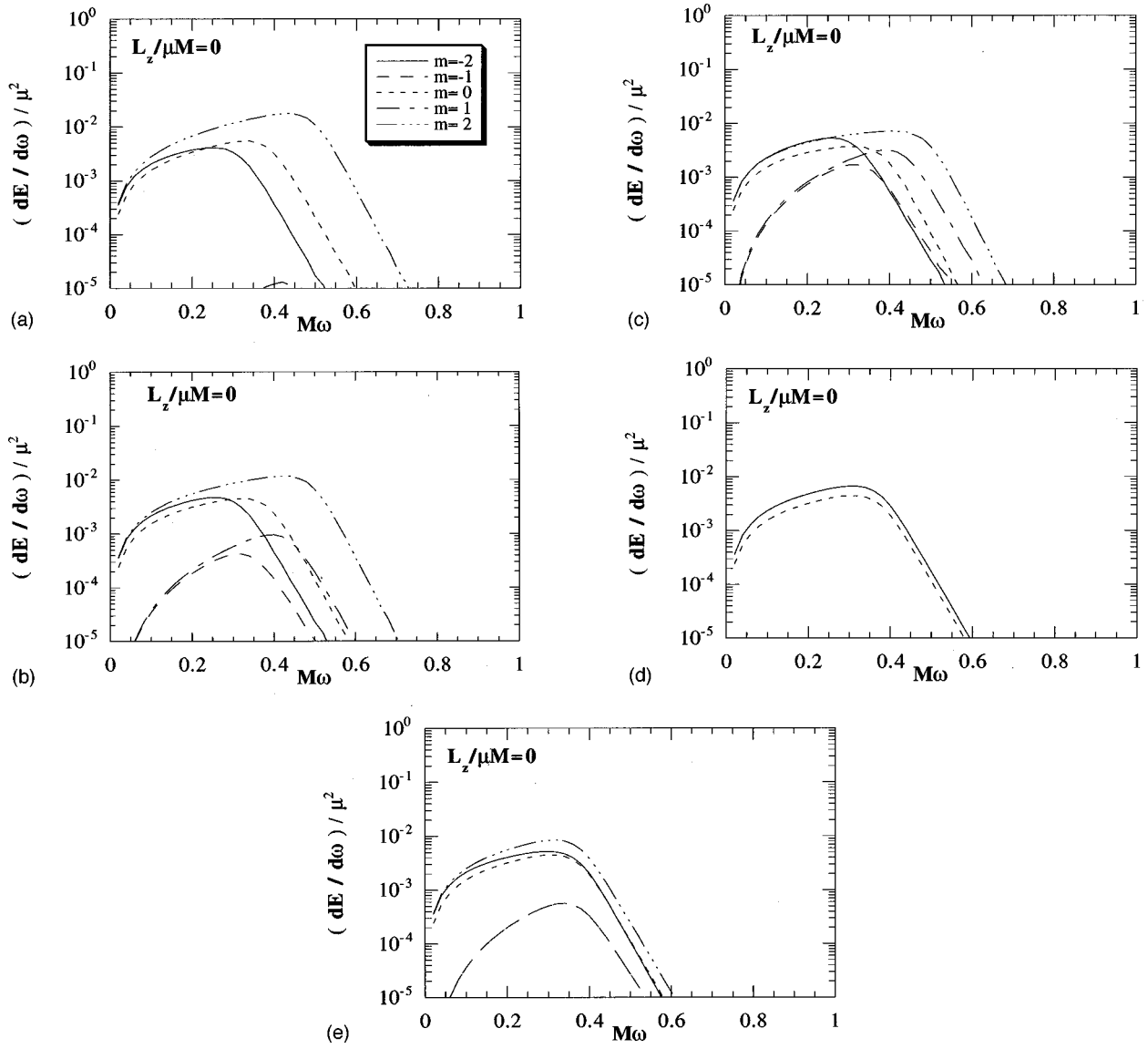

FIG. 6. The energy spectrum of emitted gravitational waves of the $l=2$ mode for the case of $a/M=0.6$ and $L_z/\mu M=0$ [(a) $(a/M,s/M)=(0.6,0.6)$, (b) $(0.6,0)$, (c) $(0.6,-0.6)$], (d) $(0,0)$, (e) $(0,0.6)$). Solid, dashed, dotted, dash-dotted, and dash-three dotted lines denote the cases of $m=-2$, -1, 0, 1, and 2, respectively.

From Figs. 5, one may find that for $L_z/\mu M=2.5>0$, the $m=l=2$ mode is always dominant. The spin parameter s is not so important in determining features of the energy spectrum, e.g., the peak amplitude and the frequency at the peak. However, we find that the amplitude of $m=2$ $(m=-2)$ mode is enhanced (suppressed) for increasing $s(>0)$, and that the amplitude of $m=2$ mode is suppressed for decreasing $s(<0)$. These features are considered as follows: With increasing J_z, the amplitude of $m=2$ $(m=-2)$ mode is enhanced (suppressed). J_z is increased either by L_z or by s. Thus, if s is positive, J_z is increased, and as a result, the amplitude of $m=2$ $(m=-2)$ mode is enhanced (suppressed). Similar feature can be found for $m=\pm 1$ modes; i.e., for positive (negative) s, the amplitude of $m=1$ mode is enhanced (suppressed), and that of $m=-1$ mode is suppressed (enhanced). On the other hand, for $L_z/\mu M=-1.5<0$, we have opposite features to those for $L_z/\mu M=2.5$, i.e., the $m=-l=-2$ mode is dominant and it is enhanced with decreasing s.

From Figs. 6 $(L_z=0)$, we may see the SS coupling effect more clearly because the SO coupling effect is suppressed. The contribution of the $m=l=2$ mode is slightly larger than that of the $m=-l=-2$ mode for $s=a$ case, while contributions of $m=l=2$ and $m=-l=-2$ modes are almost the same for $s=-a$ case. Recall that the contributions of $m=l=2$ and $m=-l=-2$ modes for $a=s=L_z=0$ are exactly the same because the system has an inversion symmetry with respect to the equatorial plane. Hence, the feature seen in the $s=-a$ case would be explained by some cancellation of some effects regarding a and s.

In Fig. 12, we show the energy spectrum of each l mode. In all the cases, the $l=2$ mode dominates the total amplitude. From Fig. 12(a), however, we find the contribution of large l modes become significant for $L_z>0$. This shows that for

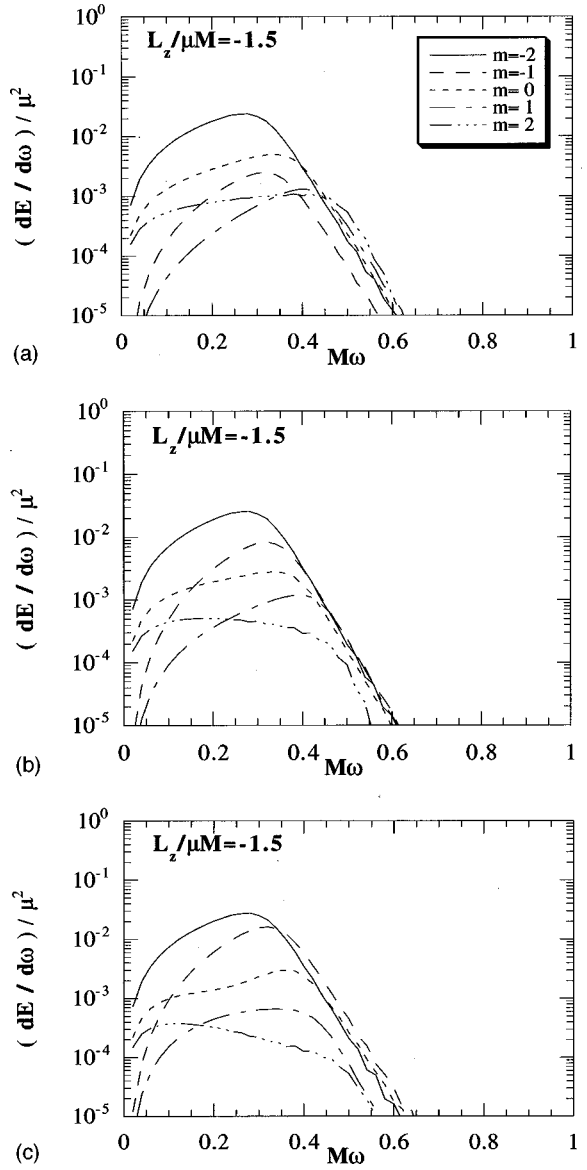

FIG. 7. The energy spectrum of gravitational waves of the $l=2$ mode for the case of $a/M=0.6$ and $L_z/\mu M=-1.5$ [(a) $s/M=0.6$, (b) $s/M=0$, (c) $s/M=-0.6$]. Solid, dashed, dotted, dash-dotted, and dash-three dotted lines denote the cases of $m=-2$, -1, 0, 1, and 2, respectively.

corotating cases $[(a\cdot L_z)>0]$, $l=m$ modes are efficiently enhanced. As for the effect of a particle spin s, we can see two clear features: If s and L_z is parallel, the emissivity of gravitational waves is enhanced and in the opposite case, it is suppressed, as we mentioned above. In addition to this, from Figs. 12(a) and (b), as the coupling $(s\cdot L_z)$ or $(s\cdot a)$ become larger, the higher l modes are enhanced more efficiently. This feature seems to imply that these SO and SS couplings excite the higher l modes.

In Figs. 13 and 14, we show waveforms of gravitational waves. We here present the waveform of the $l=2$ mode because the contribution of the higher l modes is at most $\sim 10\%$ as shown in Fig. 12. We set the observer at infinity in the direction of $\theta=\pi/2$, $\varphi=0$ for Fig. 13, and in the z axis for Fig. 14. In Fig. 13, the cross mode ($h_\times$) of gravitational waves disappears from the character of polarization.

As we mentioned in Sec. III A, gravitational waves are most efficiently radiated in the quasinormal mode ringing. In fact, we can find the damping oscillation of a quasinormal mode ringing of the significant amplitude in Figs. 13 and 14. From Figs. 13(a) and 14, it is found that the $m=l$ mode dominates over other modes for $L_z>0$ and the damping oscillation can be described by this single quasinormal mode. However when $L_z\leqslant 0$, to perform accurate fitting for the ringing tail, we need more than two quasinormal modes because the contributions of several m modes become comparable. As shown in Figs. 13(b) and 13(c), we can actually see that the ringing tail of the waveform looks different from that in Figs. 13(a) and 14.

As we mentioned above, the effect of s is not as remarkable as that of L_z, which can also be seen in Figs. 13 and 14. Even a significant change of s does not modify the waveform so much [24], however, the amplitude changes by a factor of ~ 2 for $s\lesssim M$. Thus, we cannot neglect the effect of s on the amplitude of gravitational waves although the global shape of waveforms does not change.

IV. CONCLUSION

We have calculated gravitational waves from a spinning particle moving on the equatorial plane plunging into a Kerr BH using a BH perturbation approach. We obtain the following conclusions.

Contribution of a particle spin s to the total radiated energy, linear momentum, and angular momentum of gravitational waves is not as large as that of a orbital angular momentum L_z and spin of Kerr BH a. But the effect is still important; for example, the total radiated energy changes by a factor of ~ 2 even for Kerr BH cases when magnitudes of a and L_z are moderately large, if we change s from 0 to $\lesssim M$.

Among effects due to particle spin s, SO coupling (the coupling between s and L_z) seems most important, and in the case where s and L_z are parallel (antiparallel), the amount of gravitational radiation is enhanced (suppressed). One of the main reasons is that for the parallel (antiparallel) case, the duration of the particle staying near BH horizon becomes longer (shorter) than that for the $s=0$ case due to the repulsive nature of the SO coupling force.

The reason why the effect of s is less important than that of L_z is thought that the ratio of the order of magnitude of the SO coupling to the centrifugal one is $|s|M/|L_z|r$. Thus, for $|s|\sim|L_z|$, the effect of L_z is always stronger than that of s.

The coupling effect between s and L_z is enlarged for larger a. This may indicate the importance of the coupling between a and $(s\cdot L_z)$.

The coupling between s and a is not as important as that between s and L_z, but it has still an important contribution. As in the case of the SO coupling, the total radiated energy is enhanced for the case, where s and a are parallel. This behavior is opposite to that for the case when the spinning particle falls along the spin axis of Kerr BH [13]. Thus, the amount of gravitational radiation does not simply depend on

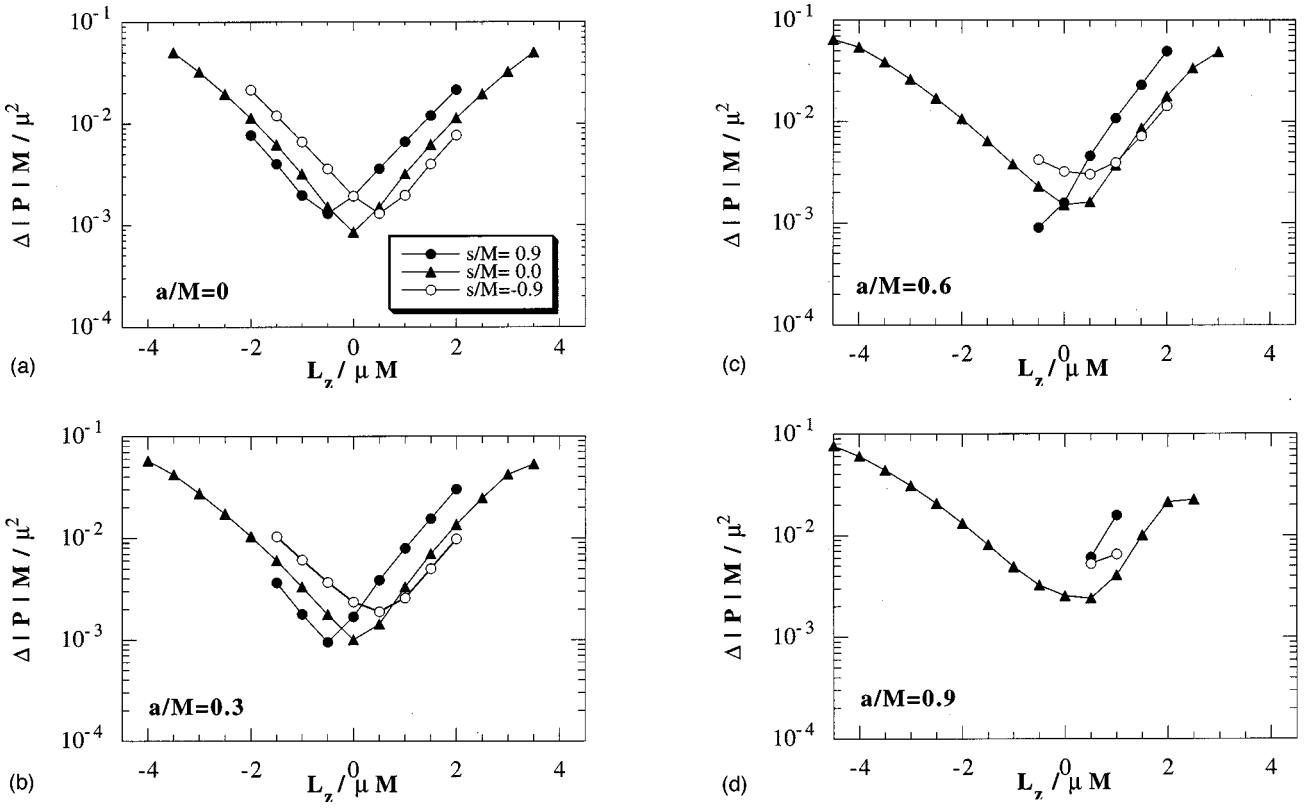

FIG. 8. The total radiated linear momentum of gravitational waves as a function of L_z [(a) $a/M=0$, (b) $a/M=0.3$, (c) $a/M=0.6$, and (d) $a/M=0.9$]. Circle (filled), triangle (filled), and circle (open) denote the cases of $s/M=0.9$, 0, and -0.9, respectively.

the direction of s, but on the type of the orbital trajectory.

The amount of gravitational radiation is maximum when the directions of axes of s, a, and L_z have a coincidence. Thus, our calculations indicate that in the coalescences of two BHs, gravitational waves are emitted most efficiently when directions of their spins and orbital angular momentum have a coincidence.

ACKNOWLEDGMENTS

We would like to thank Takashi Nakamura, Misao Sasaki, Shingo Suzuki, and Takahiro Tanaka for discussions. We also would like to thank Paul Haines for reading of our manuscript. M. Saijo thanks the JSPS Research program for Young Scientists, through Grant No. 5689 for the financial support. The numerical computations are mainly performed by the NEC-SX4 vector computer at Yukawa Institute for Theoretical Physics and in part by the FUJITSU-VX vector computer at Media Network Center, Waseda University. This work was supported partially by a Grant-in-Aid for Scientific Research Fund of the Ministry of Education, Culture, Science and Sports (Nos. 08102010, 08NP0801, and 09740336), by a JSPS Grant-in-Aid (No. 053769), and by the Waseda University Grant for Special Research Projects.

APPENDIX: GENERALIZED REGGE-WHEELER EQUATIONS AND SOURCE TERMS OF A SPINNING PARTICLE

Let us begin with a brief review of a BH perturbation approach. In order to calculate metric perturbations in a Kerr spacetime, we adopt the Sasaki-Nakamura formalism [11], which is derived by a transformation from the Teukolsky equation [12]. The radial wave equation in the Sasaki-Nakamura formalism is

$$\left(\frac{d^2}{dr^{*2}}-F(r)\frac{d}{dr^*}-U(r)\right)X_{lm\omega}(r)=\mathcal{S}_{lm\omega}(r), \quad \text{(A1)}$$

where the tortoise coordinate r^* is defined as

$$dr^*=\frac{r^2+a^2}{\Delta}dr, \quad \text{(A2)}$$

and

$$F(r)=\frac{\Delta}{r^2+a^2}\frac{1}{\gamma}\frac{d\gamma}{dr},$$

$$U(r)=G^2-FG+\frac{\Delta}{(r^2+a^2)}\frac{dG}{dr}+\frac{\Delta}{(r^2+a^2)^2}U_1,$$

with

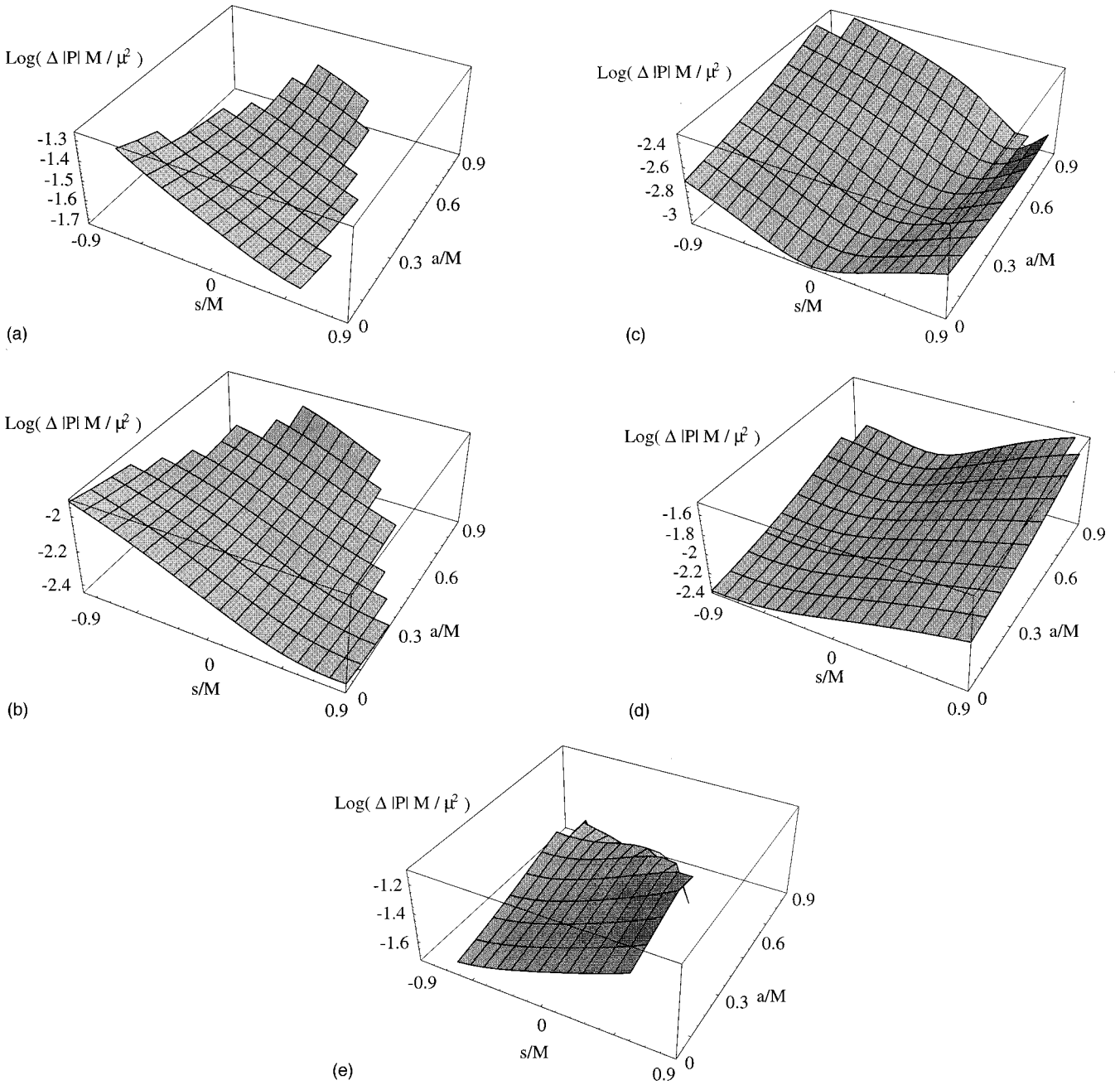

FIG. 9. The total radiated linear momentum of gravitational waves as a function of a BH spin a and a particle spin s [(a) $L_z/\mu M=-3$, (b) $L_z/\mu M=-1.5$, (c) $L_z/\mu M=0$, (d) $L_z/\mu M=1.5$, and (e) $L_z/\mu M=3$].

$$\gamma(r)=c_0+\frac{c_1}{r}+\frac{c_2}{r^2}+\frac{c_3}{r^3}+\frac{c_4}{r^4},$$

$$c_0=-12iM\omega+\lambda(\lambda+2)-12a\omega(a\omega-m),$$

$$c_1=8ia[3a\omega-\lambda(a\omega-m)],$$

$$c_2=-24iaM(a\omega-m)+12a^2[1-2(a\omega-m)^2],$$

$$c_3=24ia^3(a\omega-m)-24Ma^2,$$

$$c_4=12a^4,$$

$$G(r)=-\frac{1}{r^2+a^2}\frac{d\Delta}{dr}+\frac{r\Delta}{(r^2+a^2)^2},$$

$$U_1(r)=V_T+\frac{\Delta^2}{\beta}\left[\frac{d}{dr}\left(2\alpha+\frac{d\beta/dr}{\Delta}\right)-\frac{d\gamma/dr}{\gamma}\left(\alpha+\frac{d\beta/dr}{\Delta}\right)\right],$$

$$\alpha=-i\frac{K\beta}{\Delta^2}+3i\frac{dK}{dr}+\lambda+\frac{6\Delta}{r^2},$$

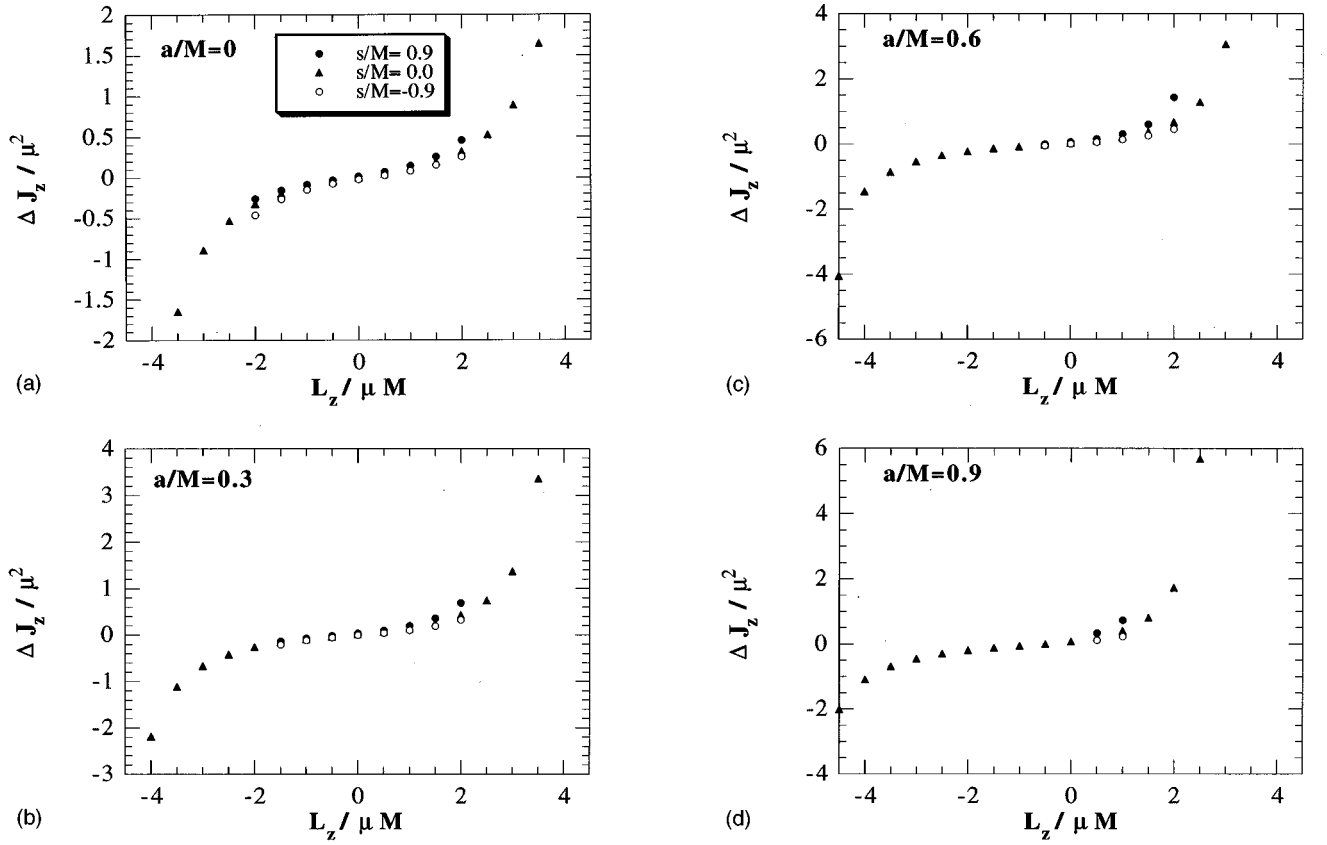

FIG. 10. The total radiated angular momentum of gravitational waves as a function of L_z[(a) $a/M=0$, (b) $a/M=0.3$, (c) $a/M=0.6$, and (d) $a/M=0.9$]. Circle (filled), triangle (filled), and circle (open) denote the cases of $s/M=0.9$, 0, and -0.9, respectively.

$$\beta=2\Delta\left(-iK+r-M-\frac{2\Delta}{r}\right).$$

V_T is the potential in the Teukolsky equation, which is given as

$$V_T(r)=-\frac{K^2+4i(r-M)K}{\Delta}+8i\omega r+\lambda, \tag{A3}$$

where $K=(r^2+a^2)\omega-ma$ and λ is the eigenvalue of the spheroidal harmonics (see below). The explicit form of the source term $\mathcal{S}_{lm\omega}(r)$ for the general motion of a spinning particle is shown below.

To describe the wave function $X_{lm\omega}(r)$ of Eq. (A1) using the Green's function method, we need two independent homogeneous solutions of the Sasaki-Nakamura equation, i.e.,

$$X^{\mathrm{in}(0)}_{lm\omega}(r)=\begin{cases} e^{-ikr^*} & \text{as } r^*\to-\infty, \\ A^{\mathrm{in}}_{lm\omega}e^{-i\omega r^*}+A^{\mathrm{out}}_{lm\omega}e^{i\omega r^*} & \text{as } r^*\to\infty, \end{cases}$$

$$X^{\mathrm{out}(0)}_{lm\omega}(r)=\begin{cases} B^{\mathrm{in}}_{lm\omega}e^{-ikr^*}+B^{\mathrm{out}}_{lm\omega}e^{ikr^*} & \text{as } r^*\to-\infty, \\ e^{i\omega r^*} & \text{as } r^*\to\infty, \end{cases}$$

where $k=\omega-ma/2r_H$ and the Wronskian W becomes

$$W\equiv X^{\mathrm{in}(0)}_{lm\omega}\frac{dX^{\mathrm{out}(0)}_{lm\omega}}{dr^*}-X^{\mathrm{out}(0)}_{lm\omega}\frac{dX^{\mathrm{in}(0)}_{lm\omega}}{dr^*}=2i\omega A^{\mathrm{in}}_{lm\omega}\frac{\gamma}{c_0}.$$

Then the inhomogeneous solution of Eq. (A1) becomes

$$X_{lm\omega}(r)=X^{\mathrm{in}(0)}_{lm\omega}\int_{r^*}^{\infty}\frac{\mathcal{S}_{lm\omega}(r)}{W}X^{\mathrm{out}(0)}_{lm\omega}dr^* + X^{\mathrm{out}(0)}_{lm\omega}\int_{-\infty}^{r^*}\frac{\mathcal{S}_{lm\omega}(r)}{W}X^{\mathrm{in}(0)}_{lm\omega}dr^*.$$

For observational point of view, we only need to know the asymptotic behavior of the wave function $X_{lm\omega}(r)$ at infinity, which is

$$X^{(\infty)}_{lm\omega}(r)=A^{(\infty)}_{lm\omega}e^{i\omega r^*}, \tag{A4}$$

where

$$A^{(\infty)}_{lm\omega}=\frac{c_0}{2i\omega A^{\mathrm{in}}_{lm\omega}}\int_{-\infty}^{\infty}\frac{\mathcal{S}_{lm\omega}(r)}{\gamma}X^{\mathrm{in}(0)}_{lm\omega}(r)dr^*. \tag{A5}$$

Then the waveform at infinity becomes

$$h_+-ih_\times=\frac{8}{r}\int_{-\infty}^{\infty}d\omega e^{i\omega(r^*-t)}\sum_{l,m}\frac{A^{(\infty)}_{lm\omega}}{c_0}-2\mathcal{S}^{a\omega}_{lm}(\theta)\frac{e^{im\varphi}}{\sqrt{2\pi}}, \tag{A6}$$

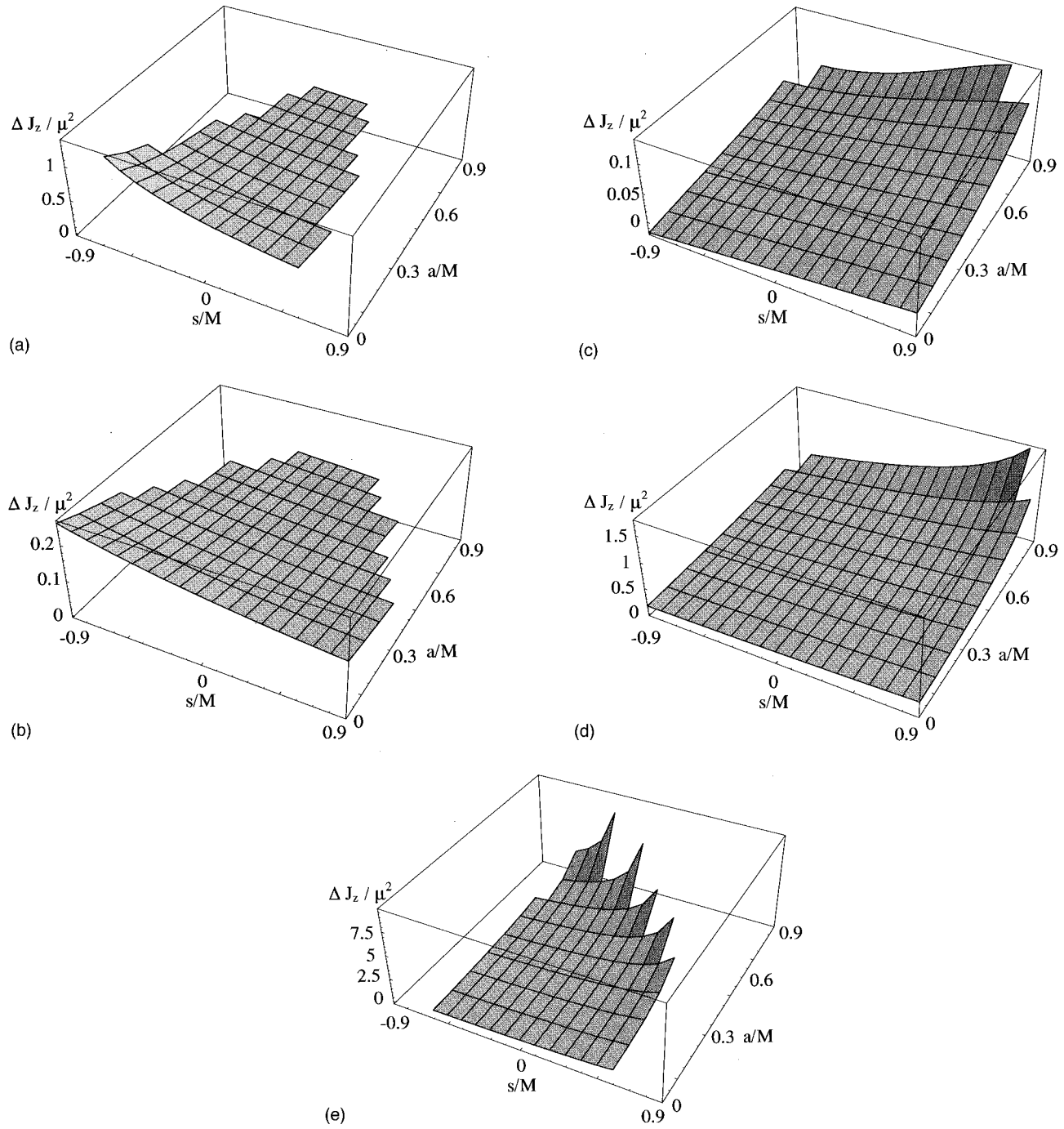

FIG. 11. The total radiated angular momentum of gravitational waves as a function of a BH spin a and a particle spin s [(a) $L_z/\mu M=-3$, (b) $L_z/\mu M=-1.5$, (c) $L_z/\mu M=0$, (d) $L_z/\mu M=1.5$ and (e) $L_z/\mu M=3$].

where ${}_{-2}S_{lm}^{a\omega}(\theta)$ is one of the spin-weighted spheroidal function, which obeys

$$\left[\frac{1}{\sin\theta}\frac{d}{d\theta}\left(\sin\theta\frac{d}{d\theta}\right)-\left(a^2\omega^2\sin^2\theta+\frac{(m-2\cos\theta)^2}{\sin^2\theta}-4a\omega\cos\theta+2-2am\omega-\lambda\right)\right]_{-2}\times S_{lm}^{a\omega}(\theta)=0. \tag{A7}$$

The spin-weighted spheroidal function ${}_{-2}S_{lm}^{a\omega}(\theta)$ is normalized as

$$\int_0^\pi d\theta\,\sin\theta\,|{}_{-2}S_{lm}^{a\omega}(\theta)|^2=1.$$

From Eq. (A6), we find the total energy, total linear momentum, total angular momentum, energy spectrum, linear momentum spectrum, and angular momentum spectrum of emitted gravitational waves are given as

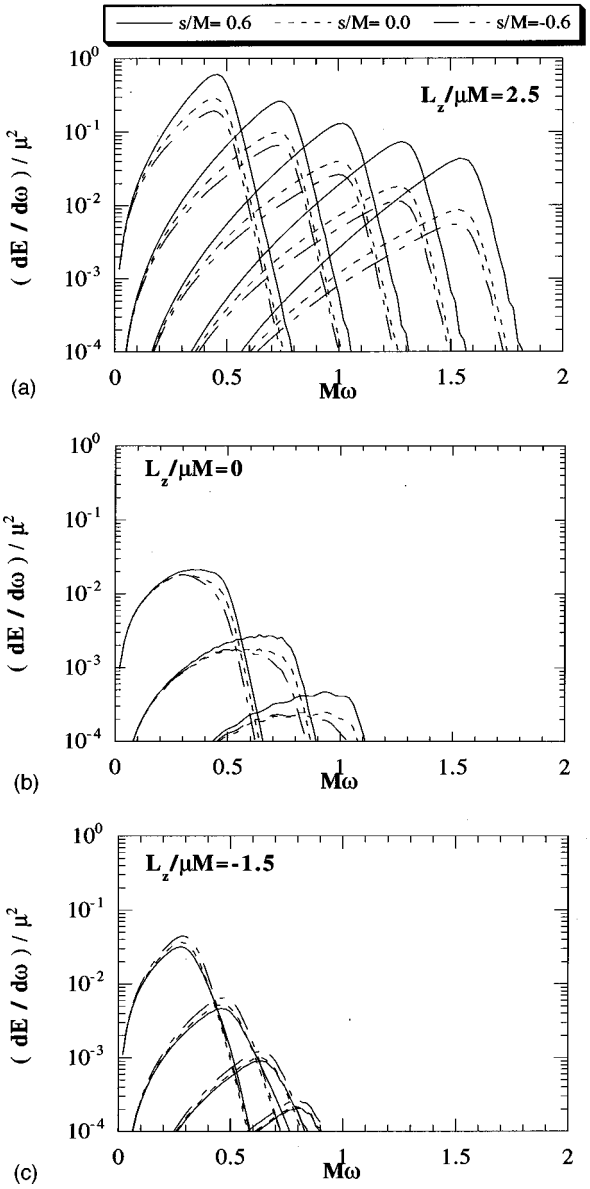

FIG. 12. The energy spectrum of gravitational waves of each l mode for the case of $a/M=0.6$ [(a) $L_z/\mu M=2.5$, (b) $L_z/\mu M=0$, (c) $L_z/\mu M=-1.5$]. Solid, dashed, and dash-dotted lines denote the cases of $s/M=0.6$, 0, and -0.6, respectively.

$$\Delta E=\int_{-\infty}^{\infty}d\omega\sum_{l,m}\left(\frac{dE}{d\omega}\right)_{lm\omega},\quad \Delta P=\int_{0}^{\infty}d\omega\sum_{l,m}\left(\frac{dP}{d\omega}\right)_{lm\omega},\quad \Delta J_z=\int_{-\infty}^{\infty}d\omega\sum_{l,m}\left(\frac{dJ_z}{d\omega}\right)_{lm\omega}, \tag{A8}$$

and

$$\left(\frac{dE}{d\omega}\right)_{lm\omega}=8\omega^2\left|\frac{A^{(\infty)}_{lm\omega}}{c_0}\right|^2,$$

$$\left(\frac{dP}{d\omega}\right)_{lm\omega}=8\omega^2\sum_{l'}\left(\frac{A^{(\infty)}_{lm\omega}}{c_0}\frac{\overline{A}^{(\infty)}_{l'm+1\omega}}{\overline{c_0}}\int_0^{\pi}d\theta\,\sin^2\theta\,{}_{-2}S^{a\omega}_{lm}(\theta)\,{}_{-2}S^{a\omega}_{l'm+1}(\theta)\right.$$
$$\left.+\frac{A^{(\infty)}_{l'm-1\omega}}{c_0}\frac{\overline{A}^{(\infty)}_{lm\omega}}{\overline{c_0}}\int_0^{\pi}d\theta\,\sin^2\theta\,{}_{-2}S^{a\omega}_{l'm-1}(\theta)\,{}_{-2}S^{a\omega}_{lm}(\theta)\right), \tag{A9}$$

$$\left(\frac{dJ_z}{d\omega}\right)_{lm\omega}=8m\omega\left|\frac{A^{(\infty)}_{lm\omega}}{c_0}\right|^2,$$

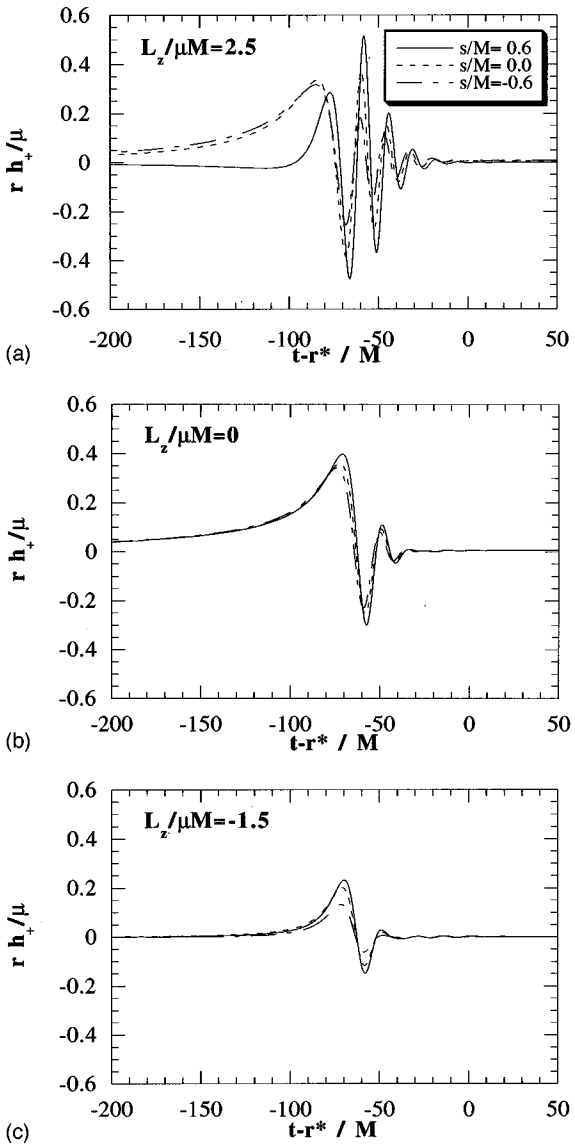

FIG. 13. The waveforms (h_+) of gravitational waves from BHs with $a/M=0.6$ [(a) $L_z/\mu M=2.5$, (b) $L_z/\mu M=0$, (c) $L_z/\mu M=-1.5$]. We only include the $l=2$ mode in the present calculation. We set the observer at infinity in the direction of $\theta=\pi/2$, $\varphi=0$ [the cross mode ($h_\times$) of gravitational wave disappears from the character of polarization]. Solid line, dashed line, and dash-dotted line correspond to the cases of $s/M=0.6$, 0, -0.6, respectively.

respectively, where we have defined a linear angular momentum by the complex valued one as $\Delta P=\Delta P_x+i\Delta P_y$.

In order to solve the Sasaki-Nakamura equation, we first have to give the source term $\mathcal{S}_{lm\omega}$ in Eq. (A1). Here we consider only nonperiodic motion or unbound system. The source term $\mathcal{S}_{lm\omega}$ is given by

$$\mathcal{S}_{lm\omega}=\frac{\gamma\Delta}{(r^2+a^2)^{3/2}r^2}\mathcal{W}\exp\left(-i\int^r\frac{K}{\Delta}dr\right). \tag{A10}$$

Here $\mathcal{W}$ is divided into three parts as

$$\mathcal{W}=\mathcal{W}_{nn}+\mathcal{W}_{mn}^{-}+\mathcal{W}_{mm}^{--}, \tag{A11}$$

$$\mathcal{W}_{nn}=f_0(r)e^{i\chi(r)}+\int_r^\infty dr' f_1(r')e^{i\chi(r')}+\int_r^\infty dr'\int_{r'}^\infty dr'' f_2(r'')e^{i\chi(r'')}, \tag{A12}$$

$$\mathcal{W}_{mn}^{-}=g_0(r)e^{i\chi(r)}+\int_r^\infty dr' g_1(r')e^{i\chi(r')}, \tag{A13}$$

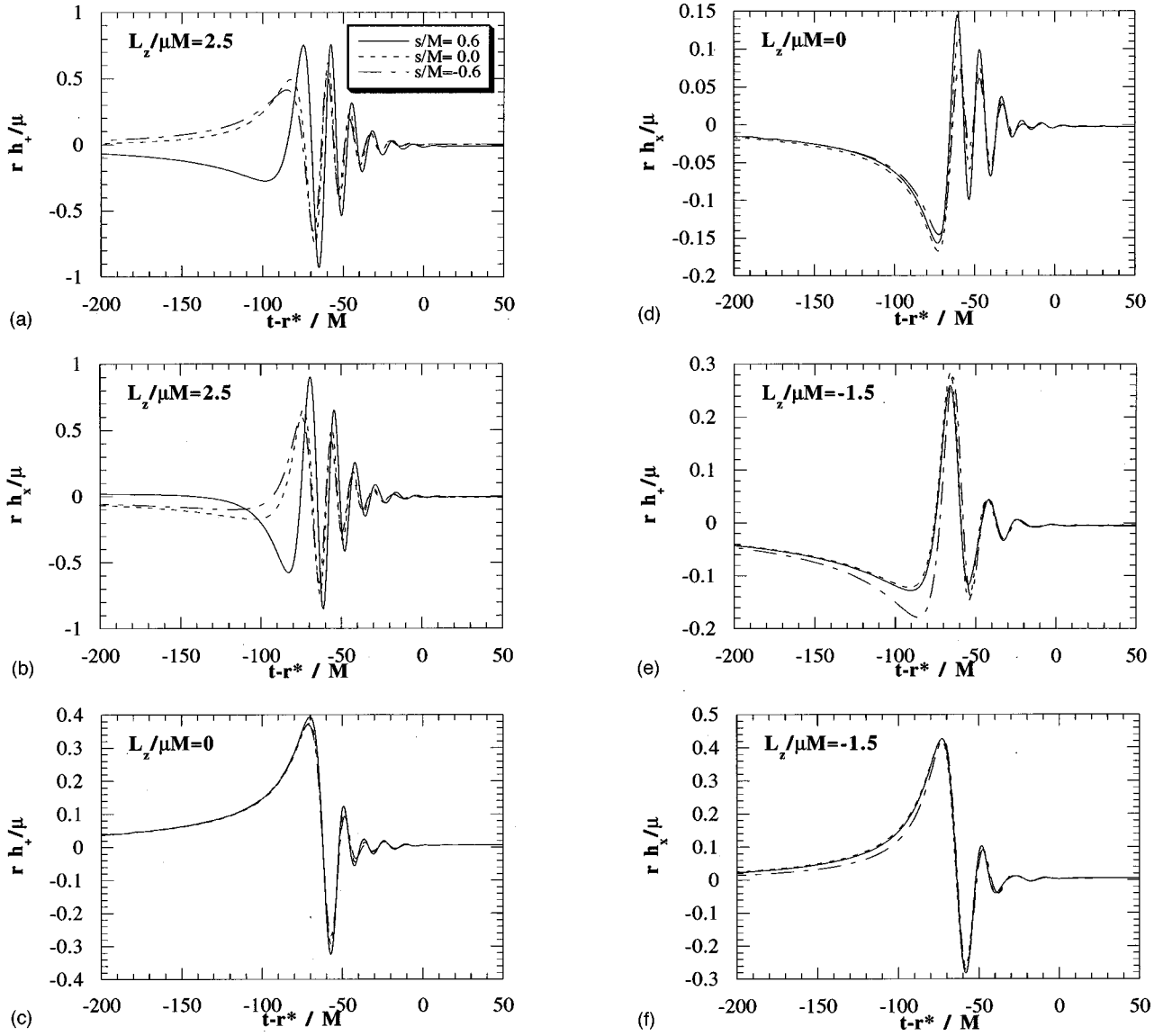

FIG. 14. The waveforms $[h_+$(a,c,e) and $h_\times$(b,d,f)] of gravitational waves from BHs with $a/M=0.6$ [(a), (b) $L_z/\mu M=2.5$, (c), (d) $L_z/\mu M=0$, (e), (f) $L_z/\mu M=-1.5$]. We only include the $l=2$ mode in the present calculation. We set the observer along the spin axis of the Kerr BH. Solid line, dashed line, and dash-dotted line correspond to the cases of $s/M=0.6,\ 0,\ -0.6$, respectively.

$$\mathcal{W}_{\overline{mm}}=h_0(r)e^{i\chi(r)}+\int_r^\infty dr' h_1(r')e^{i\chi(r')}+\int_r^\infty dr'\int_{r'}^\infty dr'' h_2(r'')e^{i\chi(r'')}, \tag{A14}$$

where

$$\chi=\omega(t+r^*)-m\tilde{\varphi}, \tag{A15}$$

$$f_0=-\frac{1}{\omega^2}w_{nn}^{(1)}-\frac{i}{\omega}w_{nn}^{(3)}, \tag{A16}$$

$$f_1=-\frac{2}{\omega^2}\left(\frac{dw_{nn}^{(1)}}{dr}+i(a\omega-m)\frac{d\tilde{\varphi}}{dr}w_{nn}^{(1)}\right)+\frac{i}{\omega}w_{nn}^{(2)}-\frac{i}{\omega}\frac{dw_{nn}^{(3)}}{dr}+(a\omega-m)\frac{w_{nn}^{(3)}}{\omega}\frac{d\tilde{\varphi}}{dr}, \tag{A17}$$

$$f_2 = -\frac{1}{\omega^2}\left\{\left[\frac{d^2 w^{(1)}_{nn}}{dr^2} + 2i(a\omega - m)\frac{d\tilde{\varphi}}{dr}\frac{dw^{(1)}_{nn}}{dr} + i(a\omega - m)\frac{d^2\tilde{\varphi}}{dr^2} w^{(1)}_{nn} - (a\omega - m)^2\left(\frac{d\tilde{\varphi}}{dr}\right)^2 w^{(1)}_{nn}\right]\right.$$
$$\left. - i\omega w^{(1)}_{nn}\left(\frac{d^2 v}{dr^2} - a\frac{d^2\tilde{\varphi}}{dr^2}\right)\right\} + \frac{i}{\omega}\frac{dw^{(2)}_{nn}}{dr} - \frac{1}{\omega}(a\omega - m)\frac{d\tilde{\varphi}}{dr} w^{(2)}_{nn}, \tag{A18}$$

$$g_0 = w^{(1)}_{mn} - \frac{i}{\omega} w^{(2)}_{mn}, \tag{A19}$$

$$g_1 = -\frac{i}{\omega}\frac{dw^{(2)}_{mn}}{dr} + (a\omega - m)\frac{w^{(2)}_{mn}}{\omega}\frac{d\tilde{\varphi}}{dr} - w^{(3)}_{mn}, \tag{A20}$$

$$h_0 = w^{(1)}_{mm} - \frac{i}{\omega} w^{(2)}_{mm} - \frac{1}{\omega^2} w^{(4)}_{mm}, \tag{A21}$$

$$h_1 = -\frac{2}{\omega^2}\left(\frac{dw^{(4)}_{mm}}{dr} + i(a\omega - m)\frac{d\tilde{\varphi}}{dr} w^{(4)}_{mm}\right) + \frac{i}{\omega} w^{(5)}_{mm} - \frac{i}{\omega}\frac{dw^{(2)}_{mm}}{dr} + (a\omega - m)\frac{w^{(2)}_{mm}}{\omega}\frac{d\tilde{\varphi}}{dr} - w^{(3)}_{mm}, \tag{A22}$$

$$h_2 = -\frac{1}{\omega^2}\left\{\left[\frac{d^2 w^{(4)}_{mm}}{dr^2} + 2i(a\omega - m)\frac{d\tilde{\varphi}}{dr}\frac{dw^{(4)}_{mm}}{dr} + i(a\omega - m)\frac{d^2\tilde{\varphi}}{dr^2} w^{(4)}_{mm} - (a\omega - m)^2\left(\frac{d\tilde{\varphi}}{dr}\right)^2 w^{(4)}_{mm}\right]\right.$$
$$\left. - i\omega w^{(4)}_{mm}\left(\frac{d^2 v}{dr^2} - a\frac{d^2\tilde{\varphi}}{dr^2}\right)\right\} + \frac{i}{\omega}\frac{dw^{(5)}_{mm}}{dr} - \frac{1}{\omega}(a\omega - m)\frac{d\tilde{\varphi}}{dr} w^{(5)}_{mm} + w^{(6)}_{mm}, \tag{A23}$$

with

$$v = t + r^*, \tag{A24}$$

$$\tilde{\varphi} = \varphi + \int^r \frac{a}{\Delta} dr, \tag{A25}$$

$$\tilde{S} = \left.\frac{d_{-2}S^{a\omega}_{lm}}{d\theta}\right|_{\theta=\frac{\pi}{2}} + (a\omega - m)_{-2}S^{a\omega}_{lm}, \tag{A26}$$

$$\hat{S} = \left(a\omega - m - i\frac{a}{r}\right)\tilde{S} - \frac{\lambda}{2}{}_{-2}S^{a\omega}_{lm}, \tag{A27}$$

$$w^{(1)}_{nn} = \frac{\sqrt{R_s}}{\Sigma_s}\hat{S}\left(1 - \frac{as}{r^2} - i\frac{s}{r}(a\omega - m)\right), \tag{A28}$$

$$w^{(2)}_{nn} = \frac{s}{\Sigma_s}[-(a+s)E + J_z]\left[\left(-\frac{r^2 - a^2}{\Delta} + \frac{3Ms^2}{r\Sigma_s}\right)\hat{S} - r\frac{d\hat{S}}{dr}\right], \tag{A29}$$

$$w^{(3)}_{nn} = s\hat{S}\frac{r}{\Sigma_s}[J_z - (a+s)E], \tag{A30}$$

$$w^{(1)}_{mn} = i\frac{s}{2}\tilde{S}\frac{r^3}{\Sigma_s\sqrt{R_s}}\left[\frac{P_s}{\Delta}(P_s - \sqrt{R_s}) + \left(1 + \frac{3Ms^2}{r\Sigma_s}\right)[J_z - (a+s)E]^2\right], \tag{A31}$$

$$w^{(2)}_{mn}=i\frac{\tilde{S}}{2}\frac{r}{\Sigma_s}\left(\left(2+\frac{3Ms^2}{r\Sigma_s}\right)r[J_z-(a+s)E]+\frac{s}{r}\left\{\frac{1}{\Delta}(r^2-3Mr+2a^2+irK)(P_s-\sqrt{R_s})\right.\right.$$
$$\left.\left.+P_s-\left[\left(4-\frac{3Ms^2}{r\Sigma_s}\right)a+i(a\omega-m)r\left(1+\frac{3Ms^2}{r\Sigma_s}\right)\right][J_z-(a+s)E]\right\}\right), \tag{A32}$$

$$w^{(3)}_{mn}=-is\frac{\tilde{S}}{2}\frac{r^2}{\Sigma_s\sqrt{R_s}}\left(1+\frac{3Ms^2}{r\Sigma_s}\right)[J_z-(a+s)E]^2, \tag{A33}$$

$$w^{(1)}_{mm}=-\frac{r^2}{2\Sigma_s\sqrt{R_s}}{}_{-2}S^{a\omega}_{lm}\left\{r^2\left(1+\frac{3Ms^2}{r\Sigma_s}\right)[J_z-(a+s)E]^2 w^{(1)}_{mm}=-\frac{r^2}{2\Sigma_s\sqrt{R_s}}{}_{-2}S^{a\omega}_{lm}\left[r^2\left(1+\frac{3Ms^2}{r\Sigma_s}\right)[J_z-(a+s)E]^2\right.\right.$$
$$\left.\left.+\left(5+ri\frac{K}{\Delta}\right)\left(1+\frac{3Ms^2}{r\Sigma_s}\right)P_s[J_z-(a+s)E]-i\frac{K}{\Delta}r\sqrt{R_s}\left(1+\frac{3Ms^2}{r\Sigma_s}\right)[J_z-(a+s)E]\right]\right\}, \tag{A34}$$

$$w^{(2)}_{mm}=-{}_{-2}S^{a\omega}_{lm}\frac{s}{r\Sigma_s}\left[a(P_s+\sqrt{R_s})+(\Delta+iKr)\left(1+\frac{3Ms^2}{r\Sigma_s}\right)[J_z-(a+s)E]\right], \tag{A35}$$

$$w^{(3)}_{mm}=\frac{r^2}{\Sigma_s\sqrt{R_s}}{}_{-2}S^{a\omega}_{lm}\left(1+\frac{3Ms^2}{r\Sigma_s}\right)[J_z-(a+s)E]\left(r[J_z-(a+s)E]+\frac{s}{r}\{2a[J_z-(a+s)E]+\sqrt{R_s}\}\right), \tag{A36}$$

$$w^{(4)}_{mm}={}_{-2}S^{a\omega}_{lm}\frac{\sqrt{R_s}as\Delta}{r^4\Sigma_s}, \tag{A37}$$

$$w^{(5)}_{mm}=-{}_{-2}S^{a\omega}_{lm}\frac{s}{r\Sigma_s}\left[2\frac{a}{r}\sqrt{R_s}+\left(\frac{\Delta}{r}+iK\right)\left(1+\frac{3Ms^2}{r\Sigma_s}\right)[J_z-(a+s)E]\right], \tag{A38}$$

$$w^{(6)}_{mm}={}_{-2}S^{a\omega}_{lm}\frac{r^2}{\Sigma_s\sqrt{R_s}}\left(1+\frac{3Ms^2}{r\Sigma_s}\right)[J_z-(a+s)E]\left([J_z-(a+s)E]-\frac{s}{r^2}\{2a[J_z-(a+s)E]-\sqrt{R_s}\}\right). \tag{A39}$$

Finally, we note that numerical methods for calculation of the radial (outgoing) waves function, the spheroidal function, and eigenvalue value λ, and so on are essentially the same as those in a previous paper [25]. When we calculate the total radiated energy, angular momentum, and linear momentum, we took the sum of l from 2 to 6.

[1] A. Abramovici, W. E. Althouse, R. W. P. Drever, Y. Gürsel, S. Kawamura, F. J. Rabb, D. Shoemaker, L. Sievers, R. E. Spero, K. S. Thorne, R. E. Vogt, R. Weiss, S. E. Whitcomb, and M. E. Zucker, Science **256**, 325 (1992).

[2] C. Bradaschia, R. D. Fabbro, A. D. Virgilio, A. Gizotto, H. Kautzky, V. Montelatici, D. Passuello, A. Brillet, O. Cregut, P. Hello, C. N. Man, P. T. Manh, A. Marraud, D. Shoemaker, F. Barone, L. D. Fiore, L. Milano, G. Russo, J. M. Aguirregabiria, H. Bel, J. P. Duruisseau, G. L. Denmat, P. Tourrenc, M. Capozzi, M. Longo, M. Lops, I. Pinto, G. Rotoli, T. Damour, S. Bonazzola, J. A. Marck, Y. Gourghoulon, L. E. Holloway, F. Fuligni, V. Iafolla, and G. Natale, Nucl. Instrum. Methods Phys. Res. A **289**, 518 (1990).

[3] J. Hough, in *Proceedings of the Sixth Marcel Grossmann Meeting*, edited by H. Sato and T. Nakamura (World Scientific, Singapore, 1992), p. 192.

[4] K. Kuroda *et al.* in *Proceedings of International Conference on Gravitational Waves: Sources and Detectors*, edited by I. Ciufolini and F. Fidecaro (World Scientific, Singapore, 1997), p. 100.

[5] E. E. Flanagan and S. A. Hughes, Phys. Rev. D **57**, 4535 (1998).

[6] R. Matzner (private communication).

[7] P. Anninos, D. Hobill, E. Seidel, L. Smarr, and W. M. Suen, Phys. Rev. Lett. **71**, 2851 (1993); Phys. Rev. D **52**, 2044 (1995).

[8] M. Davis, R. Ruffini, W. H. Press, and R. H. Price, Phys. Rev. Lett. **27**, 1466 (1971).

[9] R. Stark, in *Frontiers in Numerical Relativity*, edited by C. R. Evans, L. S. Finn, and D. W. Hobill (Cambridge University Press, Cambridge, England, 1989), p. 281 and references therein.

[10] T. Nakamura, K. Oohara, and Y. Kojima, Prog. Theor. Phys. Suppl. **90**, 171 (1987). See also references cited therein.

[11] M. Sasaki and T. Nakamura, Phys. Lett. **89A**, 68 (1982); Prog. Theor. Phys. **67**, 1788 (1982).
[12] S. A. Teukolsky, Astrophys. J. **185**, 635 (1973).
[13] Y. Mino, M. Shibata, and T. Tanaka, Phys. Rev. D **53**, 622 (1996).
[14] A. Papapetrou, Proc. R. Soc. London **A209**, 248 (1951).
[15] W. G. Dixon, in *Isolated Gravitating Systems in General Relativity*, edited by J. Ehlers (North-Holland, Amsterdam, 1979), p. 156.
[16] Note that we also have the Killing tensor in Kerr spacetime and using it, we can get other conserved quantities [17]. However, it is not necessary for the present analysis because we restrict the orbital plane of the spinning particle to the equatorial plane.
[17] T. Tanaka, Y. Mino, M. Sasaki, and M. Shibata, Phys. Rev. D **54**, 3762 (1996).
[18] C. W. Misner, K. S. Thorne, and J. A. Wheeler, *Gravitation* (Freeman, New York, 1973), p. 911.
[19] It is worth pointing out that if this condition is satisfied, Λ_s and Σ_s are always positive.
[20] R. Wald, Phys. Rev. D **6**, 406 (1972).
[21] In this subsection, the indices μ,ν are associated with the world line $z(\tau)$, while the indices α,β are associated with a field point x.
[22] B. S. DeWitt and R. W. Brehme, Ann. Phys. (N.Y.) **9**, 220 (1960).
[23] E. W. Leaver, Proc. R. Soc. London **A402**, 285 (1985). In this paper, he shows the quasinormal mode frequency of $l=2$, $m=\pm 2$ mode only in Fig. 3(c), we estimate the value from its figure.
[24] In the perturbation study, the spin angular momentum of a BH, a, is assumed to be constant even when a particle of s and L_z falls into it. In a realistic situation, however, a changes into $\sim a+s+L_z/\mu-\Delta J\mu^2/M$ and as a result, the frequency of the fundamental quasinormal mode does not agree with that of the BH before coalescence. Hence, in the case when $|s|$ and L_z/μ are as large as $|a|$, the global shape of waveform will change in reality.
[25] M. Shibata, Prog. Theor. Phys. **90**, 595 (1993).